

# Cross-Cluster Weighted Forests

Maya Ramchandran <sup>\*</sup>, Rajarshi Mukherjee, and Giovanni Parmigiani

*Abstract.* Adapting machine learning algorithms to better handle the presence of clusters or batch effects within training datasets is important across a wide variety of biological applications. This article considers the effect of ensembling Random Forest learners trained on clusters within a dataset with heterogeneity in the distribution of the features. We find that constructing ensembles of forests trained on clusters determined by algorithms such as k-means results in significant improvements in accuracy and generalizability over the traditional Random Forest algorithm. We begin with a theoretical exploration of the benefits of our novel approach, denoted as the *Cross-Cluster Weighted Forest*, and subsequently empirically examine its robustness to various data-generating scenarios and outcome models. Furthermore, we explore the influence of the data partitioning and ensemble weighting strategies on the benefits of our method over the existing paradigm. Finally, we apply our approach to cancer molecular profiling and gene expression datasets that are naturally divisible into clusters and illustrate that our approach outperforms classic Random Forest.

*Key words and phrases:* Machine learning, Random Forest, Ensemble learning, Clustering, Cancer genomics.

## 1. INTRODUCTION

Natural clusters and batch effects are common across biological and other applications, motivating the need for prediction algorithms that can adapt to cluster-like heterogeneity in the distribution of the features [11, 17]. Numerous learning algorithms have been developed for settings where the covariate-outcome relationship varies across clusters [6, 14, 22, 32]. Research has additionally suggested the possibility of improving prediction accuracy in such scenarios by partitioning data through clustering before applying a suitable ensembling approach to the pre-clustered data [13, 26, 31].

Various machine learning algorithms, including Random Forest, have been studied in relation to natural data clustering [21, 24, 28]. Itself a highly popular ensemble algorithm, Random Forest was introduced by Leo Breiman in 2001 and has since been adapted to handle a wide variety of data types and applications [3, 9, 21]. Ramchandran et al. (2020) demonstrated that ensembles of Random Forests trained on heterogeneous datasets or partitions of a large dataset outperformed single forests trained on the entire data [26]. This aligns with the multi-study ensembling approach introduced by Patil (2018),

in which effective cross-study performance is achieved by stacking learners each trained on separate studies [24]. These findings suggest that for datasets with cluster-like heterogeneity, partitioning data using clustering algorithms and to form ensembles of forests may outperform the classic Random Forest algorithm. This hypothesis forms the basis of our investigation.

This paper examines scenarios where the outcome model remains constant across clusters and the primary source of heterogeneity is in the distribution of the covariates. This situation extends the classic covariate shift paradigm to additionally consider internal heterogeneity in the training data's covariate distribution [30]. We propose a strategy of training ensembles of forests in which clusters of points that produce more highly generalizable predictors are given greater influence. We distinguish between 'estimated clusters' (algorithm-derived) and 'true clusters' (from the data-generation process) throughout our analysis.

We introduce the Cross-Cluster Weighted Forest (CCWF), a learning approach designed to improve prediction performance by leveraging data heterogeneity. The method functions as follows: first, the training data is clustered using algorithms such as k-means. Next, separate Random Forests are separately trained on each cluster. Finally, stacked regression is used to assign weights to these forests based on their stability and predictive accuracy across clusters [7]. This strategy reduces within-cluster

*Department of Biostatistics, Harvard T.H. Chan School of Public Health Department of Data Science, Dana-Farber Cancer Institute*

<sup>\*</sup>Corresponding author: ramchandran.maya@gmail.com

heterogeneity while maximizing cross-cluster diversity, aligning with the ensemble learning principle of combining diverse learners to enhance generalizability [8, 14, 27]. We investigate both the theoretical and empirical properties of CCWF, demonstrating its ability to outperform standard Random Forests in a range of simulated scenarios and real biological datasets that exhibit natural clustering.

Previous research has explored using clustering algorithms to partition data and build ensemble learners, with approaches ranging from simultaneous co-clustering and model fitting to using clustering as a preprocessing step [13, 31]. Our approach extends these insights by allowing clustering algorithms to find natural substructures without specific requirements, exploring the relationship between data partitioning and model generalizability through novel ensembling weights. Unlike previous methods that require complex cluster assignment procedures and restrict the set of samples used for prediction, we focus on creating robust ensembles that can capture diverse aspects of the input space and improve predictive performance across different scenarios. Finally, previous work linking Random Forest specifically to clustering typically uses Random Forest itself as a clustering method [4, 29, 34].

This paper is organized as follows: we first present a theoretical analysis of CCWF using an analytically tractable formulation to understand the role of the bias-variance interplay in conferring the benefits of ensembling when handling clustered data. Our findings show that cluster-based ensembles of Random Forest learners consistently outperform a single Random Forest trained on the entire dataset when train and test data contain multiple clusters. We next validate CCWF empirically through experiments on datasets with cluster structure, examining the impact of each algorithmic step and demonstrating the method’s robustness across various data generation scenarios. Finally, we apply CCWF to real gene expression and clinical data with feature distribution heterogeneity, showcasing its superior performance compared to classic Random Forest.

## 2. ALGORITHM OVERVIEW

The CCWF approach is outlined in Algorithm 1. The Random Forest algorithm traditionally uses equally-weighted trees trained on bootstrap samples. Our approach introduces a non-random data partitioning step in which we break the data into  $k$  subsections, potentially improving performance when the data can be naturally clustered. We use  $k$ -means clustering for its scalability, speed, and versatility, though any clustering method could be used [5, 12, 19]. We train Random Forests on each cluster and combine the predictions of each learner using multi-study stacking, an approach that explicitly rewards cross-cluster generalizability [7, 18, 24, 26]. Given  $k$  clusters with  $n/k$  samples each, let  $\hat{\mathbb{Y}}_b$  be predictions of forest

---

### Algorithm 1 Cross-Cluster Weighed Forest (CCWF)

---

Set the number of clusters to  $k \geq 2$ ; then,

1. Partition the training set into  $k$  disjoint clusters using an unsupervised clustering algorithm using all or a subset of the features
  2. For  $b = 1, \dots, k$ 
    - Train a Random Forest on the  $k^{th}$  cluster
    - Compute predictions for all points in the training set using this Forest
  3. Compute stacked regression weights using the full dataset and all cluster-level forest predictions as features.
  4. Construct the ensemble-level prediction as a weighted average of the cluster-level predictions.
- 

$b$  on all training samples, for  $b = 1, \dots, k$ . We compute stacked regression weights by regressing the observed training outcomes  $\mathbb{Y}$  against  $[\hat{\mathbb{Y}}_1, \dots, \hat{\mathbb{Y}}_k]^T$  using L2-norm regularization and a non-negativity constraint. Hyperparameter optimization is achieved using `glmnet` in R [15].

## 3. THEORY

In this section, we examine the asymptotic risk of CCWF compared to the classic Random Forest algorithm in a setting that, while idealized, is useful to show that bias reduction is the primary mechanism through which the general cluster-based ensembling framework produces improvements for forest-based learners.

### 3.1 Notation

We denote the training data set as  $\mathcal{D}_n = (\mathbb{X}, \mathbb{Y}) \in (\mathbb{R}_{n \times S}, \mathbb{R})$ , where  $S$  represents the number of covariates in the training set and  $n$  the training sample size. The training dataset can be further expressed as  $(\mathbb{X}, \mathbb{Y}) = ([\mathbb{X}_1 \dots \mathbb{X}_k]^T, [\mathbb{Y}_1 \dots \mathbb{Y}_k])$ , where  $k$  is the number of clusters and  $(\mathbb{X}_b, \mathbb{Y}_b) \in (\mathbb{R}_{n_b \times S}, \mathbb{R})$  is training data corresponding to the  $b^{th}$  cluster for  $b = 1, \dots, k$ . We specify that  $n_b = n/k$  and that the training covariate set consists of  $k$  equally sized, non-overlapping, uniform clusters spanning the  $[0, 1]^S$  hypercube:  $\mathbb{X}_1 \stackrel{\text{i.i.d.}}{\sim} [\text{U}(0, \frac{1}{k})]^S$ ,  $\mathbb{X}_2 \stackrel{\text{i.i.d.}}{\sim} [\text{U}(\frac{1}{k}, \frac{2}{k})]^S, \dots, \mathbb{X}_k \stackrel{\text{i.i.d.}}{\sim} [\text{U}(\frac{k-1}{k}, 1)]^S$ . We can therefore represent each training sample as  $(\mathbf{x}_i, Y_i) \stackrel{\text{i.i.d.}}{\sim} (\sum_{b=1}^k A_i [\text{U}(\frac{b-1}{k}, \frac{b}{k})]^S, f(\mathbf{x}_i))$ , where  $A_i \sim \text{Multinomial}(k, n/k)$  is a multinomial random variable representing the cluster assignment of  $\mathbf{x}_i$ . The outcome  $Y_i = f(\mathbf{x}_i)$ , where we make no assumptions on the form that the function  $f(\cdot)$  takes. Test point  $(\mathbf{x}_*, Y_*)$  follows the same distribution as the training set.

*3.1.1 Centered Random Forests* We define a Random Forest as an ensemble of base regression trees

$\{f_n(\mathbf{x}_*; \theta_m, \mathcal{D}_n), m \geq 1\}$ , where  $\theta_m$  are i.i.d. copies of a randomizing variable  $\theta$  determining node splits. The forest-level prediction is  $\bar{f}_n(\mathbf{x}_*; \theta, \mathcal{D}_n) = \mathbb{E}_\theta [f_n(\mathbf{x}_*; \theta, \mathcal{D}_n)]$ , typically estimated by averaging predictions from multiple trees trained on bootstrap samples [9]. In this section, we analyze the Centered Random Forest method proposed in [10], which simplifies the original algorithm by assuming  $\theta$  is independent of the training sample  $\mathcal{D}_n$ . This excludes bootstrapping and data-dependent tree-building strategies but permits  $\theta$  to be based on a second sample  $\mathcal{D}'_n$  i.i.d.  $\mathcal{D}_n$ , enabling the splits to be optimized in a manner closely resembling how they would have been with the actual training set. We build upon the analytical work to characterize this model in Klusowski (2020) and Biau (2012), keeping our notation consistent whenever possible [2, 20].

Centered Random Forest trees are constructed over  $\log_2 c_n$  iterations, where  $c_n \geq 2$  is a user-defined parameter that possibly depends on  $n$ . Each tree is built as follows: at each node, a coordinate of  $\mathbf{x}$  is selected, with the  $j^{\text{th}}$  feature having a probability  $p_{nj} \in (0, 1)$  of being selected, and splits occur at the midpoint of the chosen coordinate. Following from Klusowski (2020),  $p_{nj} \rightarrow 1/S$  as  $n \rightarrow \infty$ . Each tree outputs the average  $Y_i$  for  $\mathbf{x}_i$  in the same leaf node partition as  $\mathbf{x}_*$ , denoted  $A_n(\mathbf{x}_*, \theta)$ . The midpoint splitting is for mathematical convenience; more complex mechanisms could be used with  $\mathcal{D}'_n$ , but would complicate the analysis without providing additional insight into ensembling strategies. The individual tree predictor can therefore be represented as  $f_n(\mathbf{x}_*; \theta, \mathcal{D}_n) = \frac{\sum_{i=1}^n Y_i \mathbb{1}\{\mathbf{x}_i \in A_n(\mathbf{x}_*, \theta)\}}{\sum_{i=1}^n \mathbb{1}\{\mathbf{x}_i \in A_n(\mathbf{x}_*, \theta)\}} \mathbb{1}\{\epsilon_n(\mathbf{x}_*, \theta)\}$ , where  $\epsilon_n(\mathbf{x}_*, \theta)$  is the event that

$\sum_{i=1}^n \mathbb{1}\{\mathbf{x}_i \in A_n(\mathbf{x}_*, \theta)\} > 0$ ; that is, that there is at least one training point that falls within the same leaf node as  $\mathbf{x}_*$ . We can then obtain the expected prediction made by the Centered Random Forest by taking the expectation of the individual tree predictors with respect to the randomizing variable  $\theta$ :

$$\bar{f}_n(\mathbf{x}_*; \theta, \mathcal{D}_n) = \sum_{i=1}^n Y_i \mathbb{E}_\theta \left[ \frac{\mathbb{1}\{\mathbf{x}_i \in A_n(\mathbf{x}_*, \theta)\}}{\sum_{i=1}^n \mathbb{1}\{\mathbf{x}_i \in A_n(\mathbf{x}_*, \theta)\}} \mathbb{1}\{\epsilon_n(\mathbf{x}_*, \theta)\} \right]$$

**3.1.2 Modeling Approaches** We shall utilize the following language convention and model definitions for the theoretical analysis. The term *Ensemble* will refer to the following strategy:

1. Train a Centered Random Forest on  $(\mathbb{X}_b, \mathbb{Y}_b)$  for each cluster  $b = 1, \dots, k$ . The predictions of each cluster-level forest on a test point  $\mathbf{x}_* = \hat{Y}_b(\mathbf{x}_*; \theta, \mathcal{D}_n)$
2. Obtain predictions for the *Ensemble* by adding the predictions of each cluster-level forest;

$$\hat{Y}_E(\mathbf{x}_*; \theta, \mathcal{D}_n) = \sum_{b=1}^k \hat{Y}_b(\mathbf{x}_*; \theta, \mathcal{D}_n)$$

Note that Centered Random Forests do not extrapolate beyond their training data, so  $\hat{Y}(\mathbf{x}_*) = 0$  if the cluster

assignment of  $\mathbf{x}_* \neq b$ . The strategy of adding each component forest in the Ensemble is analogous to stacking weights in CCWF. This is because the Ensemble's predictions inherently represent the optimal combination of single-cluster forest predictions for any given test point. Additionally, since the partitions defined by clusters in this setting are distinct across all marginal covariate distributions, the true clusters are representative of what unsupervised clustering distributions would identify as  $n \rightarrow \infty$ . Consequently, the simplifications in this setting still represent the asymptotic behavior of the CCWF algorithm.

As a baseline, we train a single Centered Random Forest on the full dataset, which we call the *Merged* in concordance with terminology used in multi-study learning [18, 24]. We denote the predictions of the *Merged* learner on test point  $\mathbf{x}_*$  as  $\hat{Y}_M(\mathbf{x}_*; \theta, \mathcal{D}_n)$ . The aim of the following section is to derive the limit of the ratio  $\frac{RMSE(\hat{Y}_E(\mathbf{x}_*))}{RMSE(\hat{Y}_M(\mathbf{x}_*))} = \frac{\sqrt{\mathbb{B}_E^2 + \mathbb{V}_E}}{\sqrt{\mathbb{B}_M^2 + \mathbb{V}_M}}$ , where we define  $\mathbb{B}_E$  and  $\mathbb{V}_E$  as the bias and variance of the *Ensemble* predictions and  $\mathbb{B}_M$  and  $\mathbb{V}_M$  as the analogous quantities for the *Merged*.

### 3.2 Asymptotic Analysis

In Lemma 3.1, we show that the *Ensemble* and *Merged* predictions can be represented as weighted averages of the training outcome values, with the choice of weights as the differentiating factor between the methods.

LEMMA 3.1. (i) For data divided into  $k$  clusters, the predictions of the  $k$  cluster-level forests within the *Ensemble* learner on new point  $\mathbf{x}_*$  can be expressed as

$$\hat{Y}_b(\mathbf{x}_*; \theta, \mathcal{D}_n) = \sum_{i=1}^n Y_i \mathbb{E}_\theta [W_{ib}(\mathbf{x}_*, \theta)]$$

where

$$W_{ib}(\mathbf{x}_*, \theta) = \frac{\mathbb{1}\{\mathbf{x}_i \in A_n(\mathbf{x}_*, \theta)\} \mathbb{1}\{\mathbf{x}_i \in [\frac{b-1}{k}, \frac{b}{k}]^S\} \mathbb{1}\{\mathbf{x}_* \in [\frac{b-1}{k}, \frac{b}{k}]^S\}}{N_b(\mathbf{x}_*, \theta)} \times \mathbb{1}\{\epsilon_{nb}(\mathbf{x}_*, \theta)\}$$

$$N_b(\mathbf{x}_*, \theta) = \sum_{i=1}^n \mathbb{1}\{\mathbf{x}_i \in A_n(\mathbf{x}_*, \theta)\} \mathbb{1}\{\mathbf{x}_i \in [\frac{b-1}{k}, \frac{b}{k}]^S\} \mathbb{1}\{\mathbf{x}_* \in [\frac{b-1}{k}, \frac{b}{k}]^S\}$$

and  $\epsilon_{nb}(\mathbf{x}_*, \theta)$  is the event that  $N_b(\mathbf{x}_*, \theta) > 0$  for  $b = 1, \dots, k$ ;  $N_b(\mathbf{x}_*, \theta)$  represents the number of total training points from  $\mathbb{X}_b$  that fall into the same partition of the test point  $\mathbf{x}_*$  given that  $\mathbf{x}_* \in [\frac{b-1}{k}, \frac{b}{k}]^S$ . Specifically, the predictions of the overall Ensemble as

$$\hat{Y}_E(\mathbf{x}_*; \theta, \mathcal{D}_n) = \sum_{i=1}^n \sum_{b=1}^k Y_i \mathbb{E}_\theta [W_{ib}(\mathbf{x}_*, \theta)]$$

$$= \sum_{i=1}^n Y_i \mathbb{E}_\theta [W_i(\mathbf{x}_*, \theta)]$$

where  $W_i(\mathbf{x}_*, \theta) = \sum_{b=1}^k W_{ib}(\mathbf{x}_*, \theta)$ .

(ii) The predictions of the Merged learner on new point  $\mathbf{x}_*$  can be expressed as

$$\hat{Y}_M(\mathbf{x}_*; \theta, \mathcal{D}_n) = \sum_{i=1}^n Y_i \mathbb{E}_\theta [H_i(\mathbf{x}_*, \theta)]$$

where  $H_i(X, \theta) = \frac{\mathbb{1}_{\{\mathbf{x}_i \in A_n(\mathbf{x}_*, \theta)\}}}{N_n(\mathbf{x}_*, \theta)} \mathbb{1}_{\{\epsilon_n(\mathbf{x}_*, \theta)\}}$  and  $N_n(\mathbf{x}_*, \theta) = \sum_{i=1}^n \mathbb{1}_{\{\mathbf{x}_i \in A_n(\mathbf{x}_*, \theta)\}}$ , the number of total training samples falling into the same box as  $\mathbf{x}_*$ . Finally,  $\epsilon_n(\mathbf{x}_*, \theta)$  is the event that  $N_n(\mathbf{x}_*, \theta) > 0$ .

To develop theoretical results regarding the performance of these two approaches, we build on Klusowski (2020) in characterizing the asymptotic behavior of the bias and variance components of the MSE for Centered Random Forests [20]. We extend upon these results to allow for clusters in the training and test data and to remove any requirement on the functional form of the outcome model  $f(\mathbf{x})$ . We note that the latter represents a significant step forward upon previous analytical work on Random Forests, which typically assume a linear or piecewise linear outcome model.

We begin by stating supplementary results that support the primary performance comparison between the *Ensemble* and the *Merged* in Theorem 3.2 below. First, we can show that the variance terms  $\mathbb{V}_E$  and  $\mathbb{V}_M \rightarrow 0$  at a rate of  $O\left(\frac{1}{n}\right)$ , the formal statement and proof of which we provide in Lemma A.3 in the Appendix. This follows directly from the results in [Klusowski (2020), Proposition 2] and its corresponding proof [20]. We further can show that the bias terms  $\mathbb{B}_E$  and  $\mathbb{B}_M$  converge to 0 at a rate greater  $O\left(\frac{1}{n}\right)$  given minimal assumptions on  $S$  and  $c_n$ , the proof of which is given in Remark A.2 in the Appendix. Therefore, we can characterize the limit of  $\frac{RMSE(\hat{Y}_E(\mathbf{x}_*))}{RMSE(\hat{Y}_M(\mathbf{x}_*))}$  by the limit of  $\frac{\mathbb{B}_E}{\mathbb{B}_M}$ ; that is, the bias terms dominate the RMSE as  $n \rightarrow \infty$ . To further characterize this ratio, we build upon [Klusowski (2020), Theorem 4], from which we can express the leading term of  $\mathbb{B}_E$  as

$\sqrt{n(n-1)\mathbb{E}_{\mathbf{x}_*, \mathcal{D}_n, \beta} [\mathbb{E}_\theta [W_1] (\hat{Y}_1(\mathbf{x}_*) - f(\mathbf{x}_*)) \mathbb{E}_\theta [W_2] (\hat{Y}_2(\mathbf{x}_*) - f(\mathbf{x}_*))]}$   
and the leading term of  $\mathbb{B}_M$  as

$\sqrt{n(n-1)\mathbb{E}_{\mathbf{x}_*, \mathcal{D}_n, \beta} [\mathbb{E}_\theta [H_1] (\hat{Y}_1(\mathbf{x}_*) - f(\mathbf{x}_*)) \mathbb{E}_\theta [H_2] (\hat{Y}_2(\mathbf{x}_*) - f(\mathbf{x}_*))]}$

for weights  $W_1, W_2, H_1$ , and  $H_2$  as defined in Lemma 3.1. We can then derive the limit of the performance ratio between the *Ensemble* and the *Merged* as presented in Theorem 3.2 below.

**THEOREM 3.2.** *Given a training set with  $n$  samples,  $S$  covariates, and  $k \geq 2$  equally-sized uniform clusters*

$\{(\mathbf{x}_i, Y_i) \stackrel{\text{i.i.d.}}{\sim} \left( \sum_{b=1}^k A_i \left[ \mathbb{U} \left( \frac{b-1}{k}, \frac{b}{k} \right) \right]^S, f(\mathbf{x}_i) \right) : i = 1, \dots, n\}$ ,

where  $A_i \sim \text{Multinomial}(k, n/k)$  is a multinomial random variable representing the cluster assignment of  $\mathbf{x}_i$ , we can represent the predictions of the *Ensemble* and the *Merged* on test point  $\mathbf{x}_* \stackrel{\text{i.i.d.}}{\sim} \sum_{b=1}^k A_* \left[ \mathbb{U} \left( \frac{b-1}{k}, \frac{b}{k} \right) \right]^d$  as  $\hat{Y}_E$  and  $\hat{Y}_M$ , respectively. As  $n \rightarrow \infty$ , the ratio of the root mean square errors corresponding to these predictions converges as follows:

$$\lim_{n \rightarrow \infty} \frac{RMSE(\hat{Y}_E(\mathbf{x}_*))}{RMSE(\hat{Y}_M(\mathbf{x}_*))} \rightarrow \frac{1}{\sqrt{2}}$$

Theorem 3.2 demonstrates that the asymptotic performance improvement of the *Ensemble* over the *Merged* is independent of the number of true clusters  $k$  for  $k \geq 2$ . To understand this phenomenon, consider that ensembling involves a trade-off: it reduces the number of samples used to train each learner (decreasing efficiency compared to the *Merged*), but it also allows each learner to focus on regions of the covariate space that better reflect the distribution of the test point, thereby improving accuracy. The proof of Theorem 3.2 decomposes the ratio  $\frac{RMSE(\hat{Y}_E(\mathbf{x}_*))}{RMSE(\hat{Y}_M(\mathbf{x}_*))}$  into two components that capture this trade-off. It shows that when these components are multiplied, terms involving  $k$  cancel out, resulting in a final ratio of  $\frac{1}{\sqrt{2}}$ . Although each learner in the *Ensemble* is trained on  $\frac{1}{k}$  times the number of samples as the *Merged*, the benefit of the *Ensemble* approach lies in its ability to more effectively parse out the heterogeneity introduced by clusters from the true covariate-outcome relationship. This advantage outweighs the loss in efficiency due to the reduced sample size as  $n \rightarrow \infty$ . To our knowledge, this work provides the first theoretical characterizations of the Random Forest algorithm that account for heterogeneous data without imposing any functional form on the outcome model  $f(\mathbf{x})$ .

Figure 1 presents simulation results illustrating Theorem 3.2's relevance to clustered data generated from three distributional paradigms: uniform, Gaussian, and Laplace. The uniform distribution simulation matches our theoretical setup, with non-overlapping clusters of width  $\frac{1}{k}$ . In contrast, the Gaussian and Laplace simulations feature overlapping clusters characterized by different location parameters and identity scale parameters. Across all distributions and the number of simulated clusters, the ratio of *Ensemble* to *Merged* RMSEs is consistently close to  $\frac{1}{\sqrt{2}}$ ; as expected, the uniform simulation exhibits a high consistency with the theory. When assumptions are violated, in the Gaussian and Laplace cases, ratios are close to  $\frac{1}{\sqrt{2}}$  as  $k$  gets large, but can deviate for smaller values. This illustrates that our analytical framework effectively captures the performance improvements of the

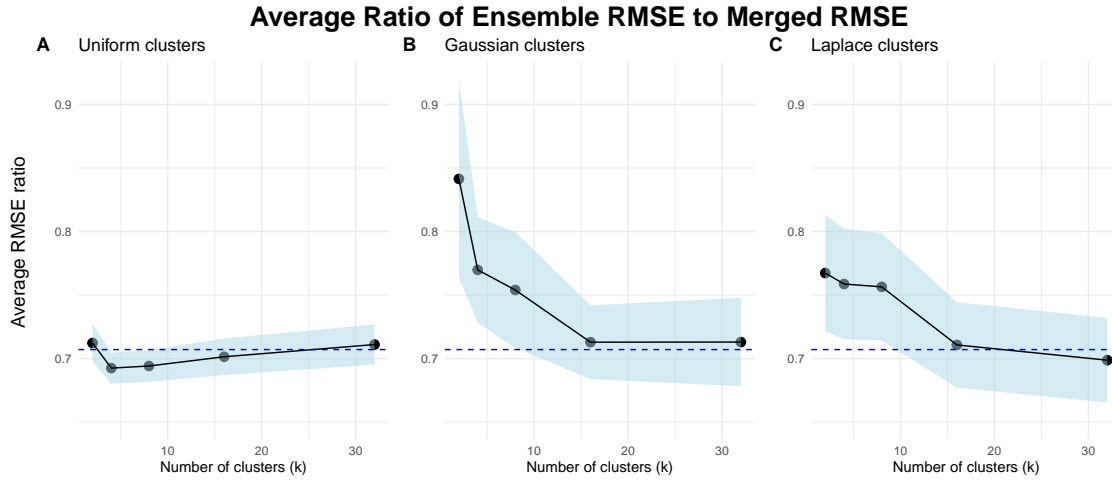


FIG 1. Average ratio of Ensemble RMSE to Merged RMSE as a function of the number of clusters in the training set ( $n = 5,000$ ). The outcome is simulated as a linear combination of 20 covariates, out of which 10 have zeroed out coefficients to induce sparsity, with added Gaussian noise. The means (points) and 95% CIs (shaded blue regions) are calculated over 150 replicates at each  $k$ . The dotted line is at the theoretical limiting ratio  $1/\sqrt{2}$ . (A) Uniform clusters (B) Multivariate Gaussian clusters (C) Multivariate Laplace clusters

Ensemble across diverse and realistic scenarios at least for large  $k$ .

## 4. SIMULATION EXPERIMENTS

### 4.1 Terminology and Setup

This section evaluates ensembling approaches on simulated data designed to mimic real genomic datasets. We first examine the importance of data partitioning on overall results, highlighting the benefits of clustering algorithms. Next, we assess the robustness of CCWF under varying conditions, including signal-to-noise ratio, number of true clusters, and sample size. We also analyze the impact of ensemble weighting strategies, comparing stacked regression weights to simple averaging and exploring how differences in ensemble weight distributions correlate with prediction accuracy. Results are averaged over 250 simulations per scenario, with 95% confidence bands computed as  $\text{mean} \pm 1.96 \times \text{standard error}$ .

We interchangeably refer to CCWF as the *Cluster* method for clarity, as this naming aligns more naturally with the other methods we compare it to. We then evaluate it alongside three variations of Algorithm 1, defined as follows. The *Random* method uses equally sized random partitions instead of clusters, keeping the number of total learners equal to  $k$ . The *Multi* method trains forests on true clusters (known in simulation but unavailable in practice) and combines them using stacking weights, resembling multi-study stacking. The *Merged* method serves as the baseline, training a single forest on the entire dataset. To ensure fair comparison, all methods are trained using the same number of total trees in order to isolate each algorithmic step’s contribution to the performance. Our approach uses 100 trees per forest for the ensemble

methods and an  $100 \times (\text{number of clusters})$  trees for the *Merged*.

We employ two methods to generate clustered datasets for our simulations: multivariate Gaussian mixture models using the R package `clusterGeneration` [25], and plasmodes more closely mimicking authentic biological clusters using the ‘monte’ function in the R package `fungible` [33]. For each of the 250 simulations per setting, we generate training data with  $n_{train}$  clusters (baseline: 5) and  $n_{test}$  test datasets with 2 clusters each (baseline: 5), all containing  $n_{coef}$  covariates (baseline: 20). We create response models by randomly selecting 10 covariates, drawing coefficients uniformly from  $[-5, -0.5] \cup [0.5, 5]$ , adding Gaussian noise, and considering non-linear relationships. Each cluster contains 500 samples at baseline, with between-cluster coefficient perturbation drawn uniformly from  $[0, 0.25]$ . Cluster separation is set at median values, allowing some overlap while remaining distinguishable. This setup enables comprehensive evaluation of feature distribution heterogeneity effects on ensemble performance across various scenarios. All modifications to this baseline strategy are outlined in the relevant results sections.

### 4.2 The Importance of Data Partitioning

We investigate how data partitioning methods affect ensemble accuracy by comparing the approaches outlined in the previous section. Both the *Cluster* and *Random* methods train component forests on the same number of partitions, but differ in how those partitions are determined. To keep notation consistent, we refer to  $k$  as the parameter used to train k-means, reflecting the number of partitions of the data also used for the *Cluster* and *Random* approaches. We explore the impact of varying  $k$

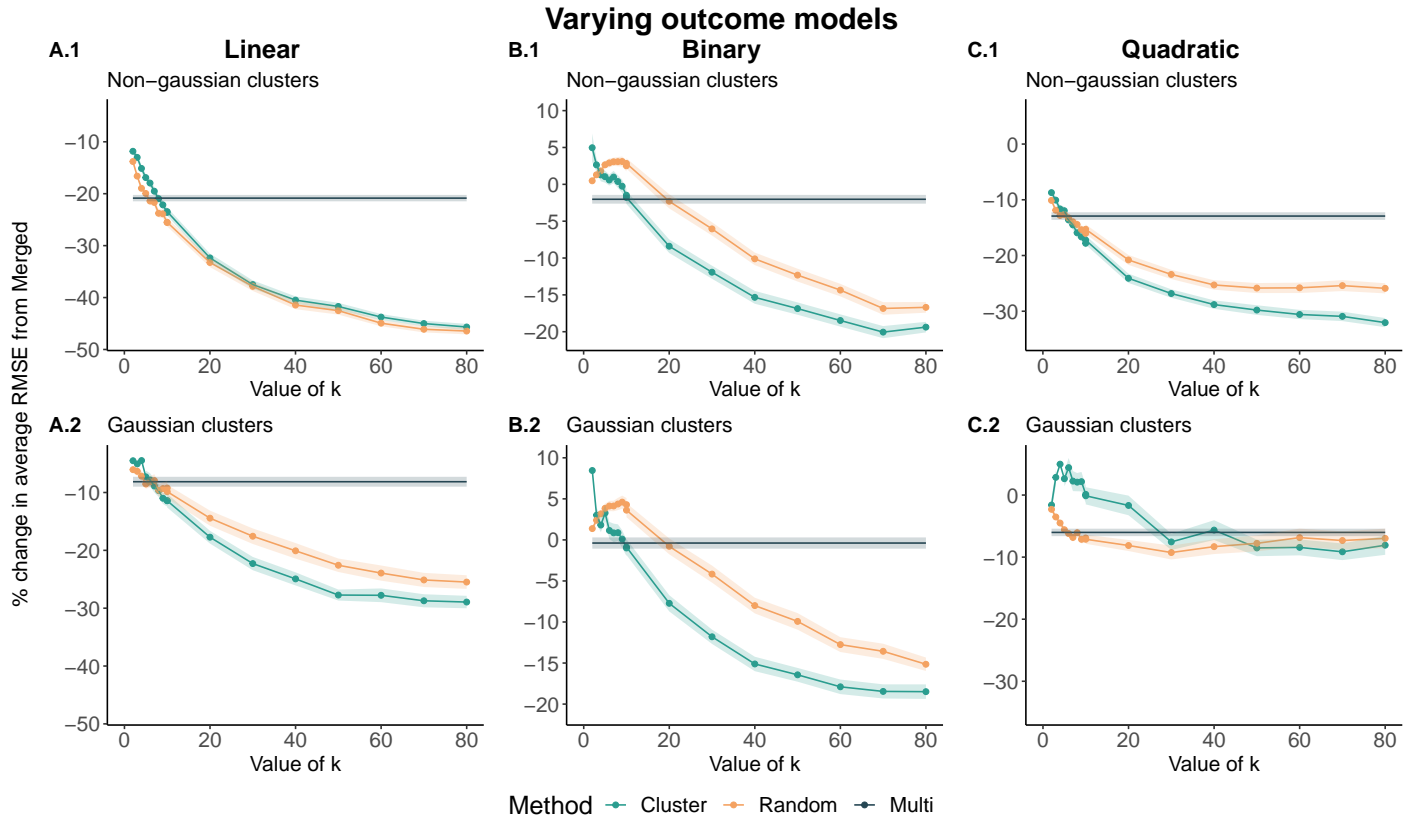


FIG 2. Percent change in average RMSE of ensembling approaches (color labeled) compared to the Merged across different data-generating scenarios, as a function of  $k$ . The first row depicts results using the non-gaussian cluster simulation approach (using the ‘monte’ function in the fungible package), while the second row uses a gaussian data generating model. (A.1-A.2) A linear model was used to generate the outcome from the covariates. (B.1-B.2) The binary outcome was created by using a cutoff from the linear model to create a binary step function. (C.1-C.2) Quadratic terms for two of the variables were added to the linear outcome-generating model.

and the data-generating mechanism across six scenarios in Figure 2.

We see that the *Cluster* and *Random* outperform the *Multi* and *Merged* when  $k$  exceeds the true number of clusters, with improvements of 20-30% at optimal values. The *Multi*, which uses true clusters, shows inconsistent performance relative to *Merged*. The *Cluster* and *Random* demonstrate robustness across different outcome models and data distributions; however, the *Cluster* generally outperforms the *Random*, suggesting k-means clustering is preferable to random partitioning. Both methods’ accuracy improves as  $k$  increases, plateauing when each forest trains on 35-40 out of 2500 observations. Correspondingly, the average tree depth decreases, indicating that high  $k$  values effectively ensemble locally weak learners akin to local smoothing approaches.

The differences between the *Cluster* and the *Random* reveal key advantages of clustering as a partitioning strategy. Increasing the number of partitions generally improves ensemble performance, with the *Multi* often outperforming other methods when  $k$  is smaller than the true number of clusters. We find a clear relationship

between prediction accuracy and covariate space range reduction: k-means partitioning achieves a lower average covariate range (3.17 CI:(3.08, 3.26)) compared to random partitioning (4.22 CI:(4.13, 4.31)), while partitioning based on the true clusters results in a significantly larger range (7.33 CI:(7.21, 7.45)). Clustering allows learners to be more uncorrelated and dissimilar, a property effective in other ensemble approaches. The improvement of the *Cluster* over the *Merged* indicates that in heterogeneous data, clustering can create more useful data partitions for training component trees. By restricting each forest to a smaller subset of the covariate space, these learners can more precisely discern subtle, localized patterns. A forest trained on observations from the distribution tails will represent those observations more comprehensively than a forest trained on the entire dataset. While clustering may result in some loss of accuracy in high-density regions for better precision in the tails, this loss does not outweigh the benefits.

Interestingly, clusters estimated by k-means do not correspond with true clusters in simulations or real genomic data (discussed in Section 5), even when  $k$

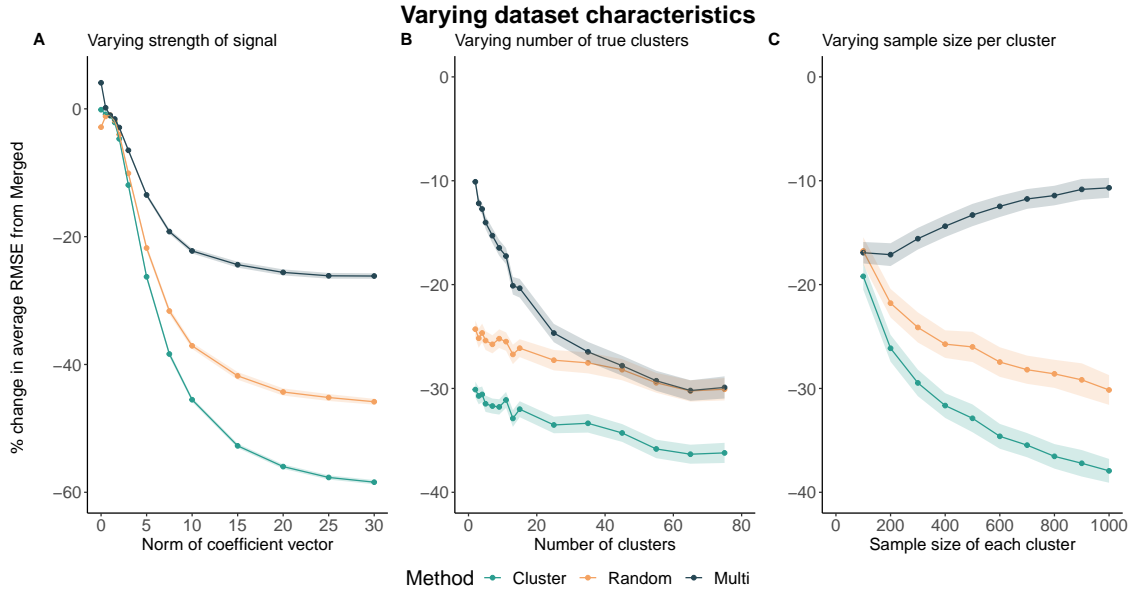


FIG 3. Percent change in average RMSE of ensembling approaches (color labeled) compared to the Merged across different data-generating scenarios. All simulations used a quadratic outcome and the non-gaussian cluster generating algorithm (using the ‘monte’ function in the fungible package). (a) Varying the magnitude of the coefficients in the outcome-generating model to examine the effect of signal strength on prediction accuracy gains. (b) Varying the number of true clusters within the training set, while keeping the total sample size constant at 2500. (c) Varying the sample size per cluster, while keeping the total number of clusters per dataset constant at 5.

equals the true cluster count. Each estimated cluster typically contains observations from all true clusters, with representation decreasing as  $k$  increases. This suggests that true clusters are not necessarily optimal for building forest ensembles. Instead, k-means’ strategy of minimizing within-cluster variance and maximizing between-cluster variance more effectively captures feature distribution heterogeneity across various data structures. This phenomenon persists in multi-study settings, where estimated clusters outperform true studies as partitions for ensemble building (see Supplement section 7.5).

Silhouette analysis, often used to determine optimal  $k$  for k-means, provides insight into CCWF’s effectiveness. The *Cluster* strategy outperforms *Merged* only when silhouette analysis indicates an optimal  $k$  greater than 1, regardless of the presence of true clusters or their separation. This observation holds across varying cluster separation levels, from mostly overlapping to completely separated. Although completely separated true clusters are unlikely to result in an optimal  $k$  of 1, CCWF’s efficacy depends more on the dataset’s suitability for unsupervised clustering than on the existence of true clusters. Similar results were observed with other clustering methods, suggesting that the unsupervised clustering step serves as a good indicator of the supervised ensembling step’s potential performance.

### 4.3 Robustness to Realistic Dataset Variety

We next evaluate method robustness across varying dataset characteristics, keeping  $k$  at the optimal value

determined by Silhouette analysis. Using a quadratic outcome model and non-Gaussian cluster generation, we examine how prediction performance is affected by covariate-outcome signal strength (by varying coefficient norms), the number of true clusters in the training set, and overall sample size.

Figure 3a shows that as covariate signal strength increases (achieved by increasing the norm of the coefficient norm in the simulated outcome model), all ensembling methods improve over *Merged*, with performance gains plateauing at 20-60%. The *Cluster* consistently outperforms others, especially at higher coefficient norms. The *Multi*’s limited improvement suggests that reducing within-cluster variation is more effective than using true clusters for discerning covariate-outcome relationships. Figure 3b demonstrates that as true cluster count increases (keeping total sample size at 2500), the *Cluster* remains superior, while the *Multi* approaches the *Random*’s performance. This occurs because *Multi*’s forest count increases with the number of true clusters, aligning with previous observations that more ensemble members improve overall accuracy even as individual model complexity decreases. The *Cluster*’s consistent advantage highlights its benefits regardless of the true data composition. Figure 3c shows that as sample size increases from 500 to 5000, the performance gap between the *Cluster* and others widens. While the *Multi* becomes less distinguishable from the *Merged* (as the *Merged* accuracy increases proportionally with sample size), the *Cluster* and *Random* continue to improve upon

No. of Clusters $K$	2	5	10	20	30	50	70	80
<b>Simple Averaging</b>	11.93	29.97	43.60	59.63	68.17	79.09	86.65	89.48
<b>Stacked Regression</b>	-9.88	-13.35	-19.73	-25.21	-27.73	-29.99	-31.96	-32.27

TABLE 1

*Simple averaging vs. stacked regression weights. Percent change in average RMSE compared to Merged for differently-weighted ensembles built on estimated clusters determined by  $k$ -means, using the non-gaussian dataset simulation framework. The first row shows results for weighting each forest equally and the second row depicts results from using stacked regression weights.*

the *Merged* since the optimal number of partitions  $k$  also increases proportionally with sample size.

#### 4.4 Importance of Ensemble Weighting Strategy

Our next simulations explore the impact of ensemble weighting strategies on prediction performance, focusing on the advantages of cross-cluster stacked regression weights over equal weighting or other approaches. We specifically highlight the importance of using cross-cluster stacked regression weights over equally weighting component learners or other weighting approaches.

Table 1 compares the percent change in average RMSE relative to the *Merged* for ensembles using simple averaging versus stacked regression weights. As  $k$  increases to its optimal value around 80, stacking-based ensembles continuously improve while equal weighting-based ensembles show declining performance. The best performance for equal weighting occurs at  $k = 2$ , at which it is still significantly worse than the *Merged*. This indicates that not all clusters from  $k$ -means produce accurate forest predictors, but certain combinations greatly outperform the *Merged*. Multi-cluster stacking up-weights the cluster-specific learners that display the best cross-cluster prediction ability. Strong cross-cluster performance suggests better learning of the true covariate-outcome relationship and greater generalizability, as clusters are designed for maximal distributional separation.

Figure 4 illustrates the distribution of stacking weights across ensembling methods using Gaussian cluster generation and a linear outcome model, with similar results achieved using non-Gaussian simulations. For each simulated dataset, the highest weight is isolated and shown in green. The *Cluster* approach most effectively up-weights beneficial predictors, indicating the presence of certain estimated clusters that produce highly generalizable forests. The *Cluster* produces weights with larger spread and a more skewed distribution compared to the *Random*, whose weights occupy a narrower, lower range. The latter is a consequence of the forests comprising the *Random* ensemble performing more similarly due to being trained on randomly selected partitions of the data. The *Multi* displays the smallest weight differences and

worst performance. Stacking indirectly re-weights each training data point’s influence on the overall predictor, with clustering aiding this process by grouping data likely to exert similar influence. The importance of including lower-weighted clusters in the ensemble is evident when comparing Ridge vs. Lasso-constrained stacking: Lasso’s removal of these clusters leads to more variable accuracy across scenarios. Ridge-constrained stacking strikes a balance, giving greater importance to up-weighted clusters while still incorporating the utility of remaining clusters, thus preventing overfitting and promoting generalizability.

## 5. DATA APPLICATION: BRAIN CANCER GENOMICS

To explore classifier performance on real biological data, we apply our methods to data on tumor samples from patients with various types of brain cancer from the Cancer Genome Atlas project (TCGA) [23]. We consider two outcomes: a binary variable indicating tumor grade and type (0 for low-grade gliomas, 1 for high-grade glioblastoma) and a continuous variable measuring the so-called mutational burden, that is the total number of DNA mutations found in the tumor. Two covariate sets are used in separate analyses: clinical data (513 patients, 50 variables, 12 of which are continuous) with missing data imputed using Random Forest via the ‘mice’ package, and gene expression data for the same patients previously shown by authors to be separable into clusters (513 patients, 100 genes). For the clinical covariates analysis, we employ the `vscoc` package in R, which uses `mclust`’s Gaussian mixture approach for simultaneous variable selection and clustering. We use `mclust`, which only handles a single data type, on the 12 continuous covariates to demonstrate the flexibility of our cluster-weighted ensemble framework to algorithms beyond  $k$ -means. Gene expression data clustering is based on the original authors’ cluster analysis.

We implement our ensembling strategies as follows: *Merged* remains a single 500-tree forest trained on all 50 covariates. *Subset Merged* refers to a single 500-tree forest trained only the 12 continuous variables. *Sample Weighted* refers to first clustering training data using `vscoc`, training 100-tree forests on each cluster,



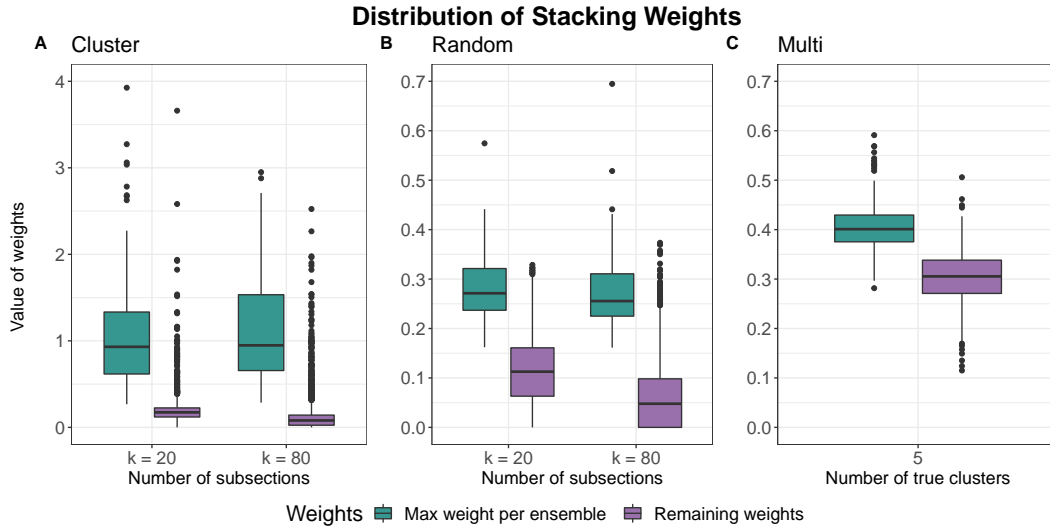


FIG 4. Distribution of the ensemble weights determined by stacked regression for (a) Cluster, (b) Random, and (c) Multi for  $k = 20$  and  $k = 80$  for the first two methods, and 5 true clusters for the latter. We used the gaussian cluster-generation framework. The distribution of the largest weight per ensemble is depicted in green, while the rest of the weights are visualized in purple. Results are shown over 100 iterations at each value of  $k$ .

and ensembling the learners with weights proportional to each cluster’s sample size. *Stack Ridge* follows the same clustering and forest-training paradigm as *Sample Weighted*, but instead ensembles learners using stacked regression weights with a ridge constraint. For each iteration, we randomly select 100 samples for testing and use the rest for training, repeating this process 500 times to obtain distributional and median prediction accuracy measures.

Figure 5 displays the results of these analyses: we observe substantial improvement of clustering methods over merging approaches across all covariate types and outcomes considered. For molecular profiling data (Fig. 5A), ensembles show 20-30% median improvement over merged-based learners in predicting mutation numbers, indicating *vsccl*’s effectiveness for ensemble cluster construction. Gene expression data (Fig. 5b) shows even more impressive improvements, with *Sample Weighted* and *Stack Ridge* achieving around 75% median improvement over the *Merged*. The gene expression clusters used to build the ensemble were previously found to align with biologically relevant characteristics [23]. While *Stack Ridge* consistently outperforms *Sample Weighted* across prediction tasks, the difference is modest, suggesting the weighting scheme’s influence on prediction ability varies by context. These results demonstrate CCWF’s robustness across different outcomes, covariates, and cluster constructions in a real biological setting.

We hypothesize that CCWF is most effective when clustering variables differ from those most associated with the outcome. This is supported by the poor performance of ensembles trained solely on clustering variables. Analysis of Random Forest variable importance rankings

for the *Subset Merged* learner showed a median 20% overlap (IQR 0-33%) between clustering variables and those important for outcome prediction, supporting our hypothesis [1]. This low overlap suggests that variables driving cluster formation are not necessarily key to predicting the outcome in this dataset. These findings illuminate the conditions under which cluster-based ensembling may surpass traditional merging approaches.

## 6. EXTENSION TO MULTIPLE STUDIES

Finally, we examine whether we can more optimally partition the total amount of data when multiple studies are available for training that measure the same covariates and outcome variable. The traditional multi-study ensembling paradigm is to train a single learner on each study and combine learners using some weighting strategy such as stacking [24]. This is analogous to the *Multi* method when we are able to separate data into its true clusters. We now explore whether training  $k$ -means on the merged data (comprising covariate data from all of the training studies) produces improvements comparatively to the single dataset setting. We furthermore evaluate the performance of these approaches on real gene expression data from the CuratedOvarianData repository from Bioconductor in R [16]. Finally, we explore whether the general strategy of ensembling learners built on clusters also works for Neural Network base learners, and compare the results to ensembles using Random Forest.

The general framework for the simulation setup used to create Figure 6 is drawn from Ramchandran et. al. (2020) [26]. We use all 15 studies in CuratedOvarianData that include survival information without any missing data in the features. For  $N = 250$  iterations per value of  $k$ , we

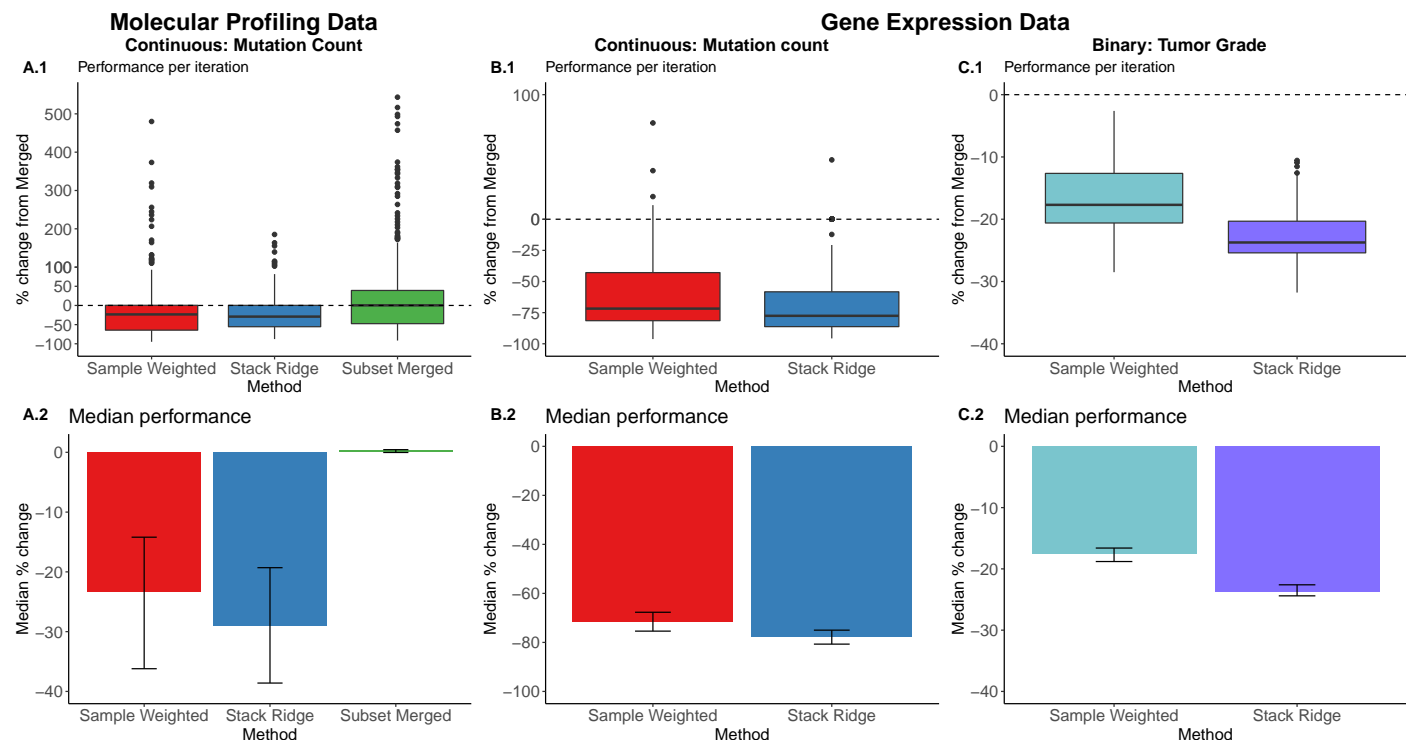


FIG 5. Percent change in average RMSE of ensembling approaches (color labeled) compared to the Merged across two sets of covariate data and two different outcomes from the LGG study. The top row shows 500 iterations of splitting the available data into training and test sets, while the second row displays the median over all iterations with associated confidence intervals. (a) Molecular profiling covariate data, mutation count outcome. (b.1) Gene expression covariate data, mutation count outcome. (b.2) Gene expression covariate data, tumor grade outcome.

randomly separate the 15 datasets from CuratedOvarianData into 10 training and 5 validation sets. We then generate the outcome using a non-linear model in order to test the ability of the candidate learning methods to detect more difficult covariate-outcome relationships. We simulate baseline levels of coefficient perturbation per study similarly to the setup discussed in Section 4.1. Using either Random Forest or Neural Nets as the base learner, we then construct ensembles using the four main approaches compared throughout this paper. The *Multi* in this case trained a learner on each study to form the final ensemble. All ensembles are built using stacked regression weights with a ridge constraint.

For Random Forest-based ensembles, clustering outperforms study-based partitioning for  $k$  greater than the number of training studies. The *Cluster* approach remains most effective, followed by *Random*, *Multi*, and the *Merged*. The true cluster or study-membership does not represent the most effective data partitioning for Random Forest; again, it is more effective to partition the data based on minimizing within-cluster heterogeneity and maximizing across. Overall, these results suggest that for either single or multiple training datasets, the *Cluster* approach should be used for Random Forest learners.

For Neural Network-based models, the *Cluster* method still produces improvements over training on true studies

or the merged data, though less so than with Random Forest. Notably, the *Cluster* approach yields similar accuracy with both base learning algorithms. While Neural Nets outperform Random Forest using the *Merged* and *Multi* approaches, the *Cluster* method elevates Random Forest-based ensembles to match Neural Net performance. This can be intuitively understood by comparing the *Cluster* strategy to convolutional neural networks, in which the estimated clusters represent the convolutional neighborhoods and the stacking weights delineate the relationship between the tree-learning and the stacking layers. While this analogy does not numerically explain the similar performance of the two algorithms, it provides insight into why we may be seeing these results.

## 7. CONCLUSIONS

In this paper, we introduce CCFWs—ensembles of forests trained on estimated clusters with weights rewarding cross-cluster performance. CCFWs yield more generalizable and accurate predictors, showing substantial gains over traditional Random Forests across theoretical analyses, simulations, and real data exhibiting feature distribution heterogeneity. We also investigate the theoretical underpinnings of the success of this approach by analyzing Centered

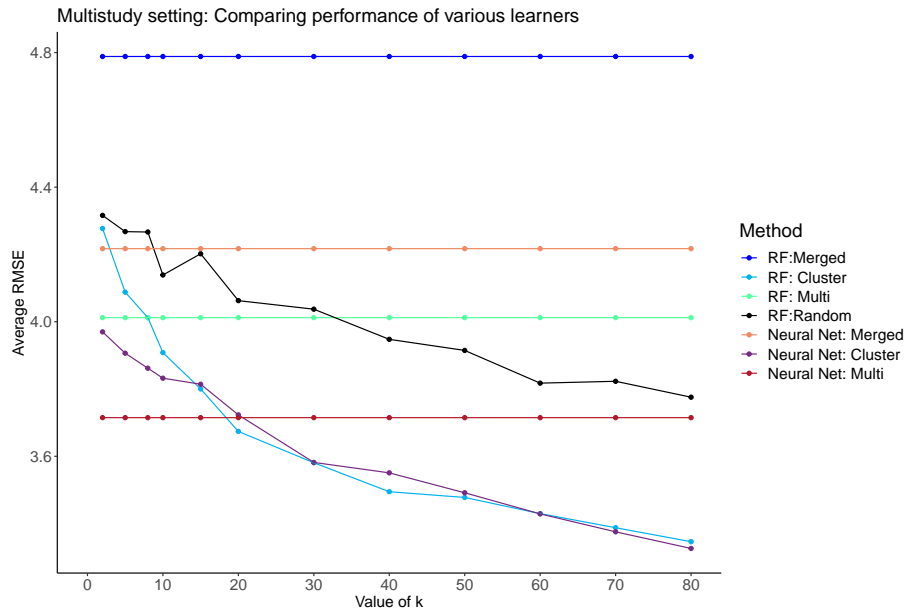


FIG 6. Average RMSE's of ensembling approaches (color labeled) as a function of  $k$  in the multi-study analysis. 20 total covariates, 10 associated with the outcome; nonlinear outcome model of the form  $y = \beta^T \mathbf{X} + 4.4x_1 - 1.8x_2 + 10 \sin(10\pi x_1)$ .

Random Forest learners in a simplified CCWF ensembling setup. We demonstrate that the benefit of ensembling over merging is to reduce the bias of the resulting predictor, supporting the empirical result from Figure 1. Furthermore, we provide an asymptotic limit of the ratio between RMSE's of the ensemble and merged predictor that imply consistent, strict improvement of ensembling over merging for clustered data. Overall, the theoretical insights support all our empirical conclusions from simulations and real data examples.

Our findings highlight the importance of data partitioning in Random Forest algorithms. Notably, dividing data based on true clusters or studies isn't always optimal. Reducing within-cluster covariate heterogeneity appears to enhance learning efficiency, even with smaller sample sizes. CCWFs can match complex Neural Net performance where traditional Random Forests fall short (Figure 6). CCWFs may effectively handle unknown batch effects by isolating subsets identified through clustering when their models don't generalize well. This approach could be particularly useful in multi-study scenarios, potentially outperforming multi-study ensembles in mitigating negative impacts of batch effects [35]. Our experiments also provide insight into the relationship between clustering variables and outcome-predictive variables: when these sets have low overlap, cluster-based ensembling tends to outperform merging approaches.

Future research should explore weighting individual trees instead of forests within ensembles. While we focused on forest weighting for clarity and generalizability, preliminary results (Figure 6) suggest tree-level weighting could further improve performance. Additional studies

could examine whether our conclusions hold under this more granular weighting approach, as demonstrated by (Ramchandran 2020) in multi-study settings [26]. Random forests are among the most widely applied machine learning tools, with thousands of published applications across a broad spectrum of data types. We have identified a simple method to provide substantial improvements. We hope that in the immediate term, this will contribute to concrete advances in predictive ability in many areas. We also believe that the architecture we outlined, as a general concept, may provide further important insight into combining simple and successful machine learning tools via multi-layer approaches.

## 8. SOFTWARE AND REPRODUCIBILITY

All code to replicate analyses from this paper can be found at <https://github.com/m-ramchandran/cross-cluster>. The CCWF method is implemented within the `rCCWF` R package at <https://github.com/m-ramchandran/rCCWF> and the `PyCCWF` Python package available through `PyPi`.

## FUNDING

Maya Ramchandran was supported by NIH-NCI Training Grant T32CA009337 at Harvard T.H. Chan School of Public Health. Rajarshi Mukherjee was partially supported by NSF Grant EAGER-1941419. Giovanni Parmigiani was supported by grant NSF-DMS 1810829.

## BIBLIOGRAPHY

- [1] ARCHER, K. J. and KIMES, R. V. (2008). Empirical characterization of random forest variable importance measures.

- Computational Statistics and Data Analysis* **52** 2249–2260. <https://doi.org/10.1016/j.csda.2007.08.015>
- [2] BIAU, G. (2012). Analysis of a Random Forests Model. *Journal of Machine Learning Research* **13** 1063–1095.
- [3] BIAU, G. and SCORNET, E. (2016). A random forest guided tour. *TEST* **25** 197–227. <https://doi.org/10.1007/s11749-016-0481-7>
- [4] BICEGO, M. (2019). K-Random Forests: a K-means style algorithm for Random Forest clustering. In *2019 International Joint Conference on Neural Networks* 1–8. <https://doi.org/10.1109/IJCNN.2019.8851820>
- [5] BOTTOU, L. and BENGIO, Y. (1995). Convergence properties of the k-means algorithms. In *Advances in Neural Information Processing Systems* 585–592.
- [6] BOUWMEESTER, W., TWISK, J. W. R., KAPPEN, T. H., VAN KLEI, W. A., MOONS, K. G. M. and VERGOUWE, Y. (2013). Prediction models for clustered data: comparison of a random intercept and standard regression model. *BMC Medical Research Methodology* **13**. <https://doi.org/10.1186/1471-2288-13-19>
- [7] BREIMAN, L. (1996). Stacked Regressions. *Machine Learning* **24** 49–64. <https://doi.org/10.1023/A:1018046112532>
- [8] BREIMAN, L. (1996). Bagging Predictors. *Machine Learning* **24** 123–140. <https://doi.org/10.1023/A:1018054314350>
- [9] BREIMAN, L. (2001). Random Forests. *Machine Learning* **45** 5–32. <https://doi.org/10.1023/A:1010933404324>
- [10] BREIMAN, L. (2004). Consistency for a simple model of random forests Technical Report, UC Berkeley.
- [11] CHAUHAN, R., KAUR, H. and ALAM, M. A. (2010). Data clustering method for discovering clusters in spatial cancer databases. *International Journal of Computer Applications* **10** 9–14.
- [12] COATES, A. and NG, A. Y. (2012). Learning feature representations with k-means. In *Neural Networks: Tricks of the Trade* 561–580. Springer.
- [13] DEODHAR, M. and GHOSH, J. (2007). A Framework for Simultaneous Co-Clustering and Learning from Complex Data. Association for Computing Machinery, New York, NY, USA.
- [14] DIETTERICH, T. G. (2000). Ensemble Methods in Machine Learning. In *Proceedings of the First International Workshop on Multiple Classifier Systems*. MCS '00 1–15. Springer-Verlag, Berlin, Heidelberg.
- [15] FRIEDMAN, J., HASTIE, T. and TIBSHIRANI, R. (2010). Regularization Paths for Generalized Linear Models via Coordinate Descent. *Journal of Statistical Software* **33** 1–22.
- [16] GANZFRIED, B. F., RIESTER, M., HAIBE-KAINS, B., RISCH, T., TYEKUCHEVA, S., JAZIC, I., WANG, X. V., AHMADIFAR, M., BIRRER, M. J., PARMIGIANI, G., HUTTENHOWER, C. and WALDRON, L. (2013). curatedOvarianData: clinically annotated data for the ovarian cancer transcriptome. *Database (Oxford)* **2013** bat013. PMID: PMC3625954. <https://doi.org/10.1093/database/bat013>
- [17] GOH, W. W. B., WANG, W. and WONG, L. (2017). Why batch effects matter in omics data, and how to avoid them. *Trends in Biotechnology* **35** 498–507.
- [18] GUAN, Z., PARMIGIANI, G. and PATIL, P. (2019). Merging versus Ensembling in Multi-Study Machine Learning: Theoretical Insight from Random Effects. *arXiv*.
- [19] HARTIGAN, J. A. and WONG, M. A. (1979). Algorithm AS 136: A k-means clustering algorithm. *Journal of the Royal Statistical Society, Series C (Applied Statistics)* **28** 100–108.
- [20] KLUSOWSKI, J. M. (2020). Sharp Analysis of a Simple Model for Random Forests. Version 4.
- [21] LIAW, A. and WIENER, M. (2002). Classification and Regression by randomForest. *R News* **2** 18–22.
- [22] LUO, J. and SCHUMACHER, M. E. A. (2010). A comparison of batch effect removal methods for enhancement of prediction performance using MAQC-II microarray gene expression data. *The Pharmacogenomics Journal* **10** 278–291. <https://doi.org/10.1038/tpj.2010.57>
- [23] CANCER GENOME ATLAS RESEARCH NETWORK (2015). Comprehensive, Integrative Genomic Analysis of Diffuse Lower-Grade Gliomas. *The New England journal of medicine* **372** 2481–2498. <https://doi.org/10.1056/NEJMoa1402121>
- [24] PATIL, P. and PARMIGIANI, G. (2018). Training replicable predictors in multiple studies. *Proceedings of the National Academy of Sciences* **115** 2578–2583. <https://doi.org/10.1073/pnas.1708283115>
- [25] QIU, W. and JOE, H. (2020). clusterGeneration: Random Cluster Generation (with Specified Degree of Separation). *R*.
- [26] RAMCHANDRAN, M., PATIL, P. and PARMIGIANI, G. (2020). Tree-Weighting for Multi-Study Ensemble Learners. *Pacific Symposium on Biocomputing* **25** 451–462. <https://doi.org/10.1101/698779>
- [27] SCHAPIRE, R. (2003). The Boosting Approach to Machine Learning: An Overview. *Nonlinear Estimation and Classification. Lecture Notes in Statistics* **171** 5–32. [https://doi.org/10.1007/978-0-387-21579-2\\_9](https://doi.org/10.1007/978-0-387-21579-2_9)
- [28] SHARKEY, A. J. C. (1996). On Combining Artificial Neural Nets. *Connection Science* **8** 299–314. <https://doi.org/10.1080/095400996116785>
- [29] SHI, T. and HORVATH, S. (2006). Unsupervised Learning With Random Forest Predictors. *Journal of Computational and Graphical Statistics* **15** 118–138. <https://doi.org/10.1198/106186006X94072>
- [30] SUGIYAMA, M., KRAULEDAT, M. and MÜLLER, K.-R. (2007). Covariate shift adaptation by importance weighted cross validation. *Journal of Machine Learning Research* **8**.
- [31] TRIVEDI, S., PARDOS, Z. A. and HEFFERNAN, N. T. (2015). The Utility of Clustering in Prediction Tasks. *CoRR abs/1509.06163*.
- [32] VERBEKE, G. and LESAFFRE, E. (1996). A linear mixed-effects model with heterogeneity in the random-effects population. *Journal of the American Statistical Association* **91** 217–221.
- [33] WALLER, N. G. (2020). fungible: Psychometric Functions from the Waller Lab. version 1.95.4.8.
- [34] YAN, D., CHEN, A. and JORDAN, M. I. (2013). Cluster Forests. *Computational Statistics and Data Analysis* **66** 178–192. <https://doi.org/10.1016/j.csda.2013.04.010>
- [35] ZHANG, Y., PATIL, P., JOHNSON, W. E. and PARMIGIANI, G. (2020). Robustifying Genomic Classifiers To Batch Effects Via Ensemble Learning. *Bioinformatics*. PMC8485848. <https://doi.org/10.1093/bioinformatics/btaa986>

## PROOFS

## A.1 Proof of Theorem 3.2

In this section, we provide a derivation for the limit of the ratio between the bias of the *Ensemble* and the bias of the *Merged* when the number of clusters in the training and testing data is equal to  $k$  for  $k \geq 2$ .

Throughout, we use the following result regarding the leaf node containing test point  $\mathbf{x}_*$ .

REMARK A.1. Let  $a_{nj}(\mathbf{x}_*, \theta)$  and  $b_{nj}(\mathbf{x}_*, \theta)$  be the left and right endpoints of  $A_{nj}(\mathbf{x}_*, \theta)$ , the  $j^{\text{th}}$  side of the box containing  $\mathbf{x}_*$ , for  $j = 1, \dots, S$ . For ease of notation, we will henceforth refer to  $a_{nj}(\mathbf{x}_*, \theta)$  as  $a_{nj}$  and  $b_{nj}(\mathbf{x}_*, \theta)$  as  $b_{nj}$ .  $c_{nj}(\mathbf{x}_*, \theta)$  represents the number of times that the  $j^{\text{th}}$  coordinate is split, with the total number of splits across all coordinates set to equal  $\log_2 c_n$  for some constant  $c_n > 2$ . For ease of notation, we will suppress the dependencies of  $a_{nj}$ ,  $b_{nj}$ , and  $c_{nj}$  on  $(\mathbf{x}_*, \theta)$ . We then observe that each endpoint of  $A_{nj}(\mathbf{x}_*, \theta)$  is a randomly stopped binary expansion of  $\mathbf{x}_*^{(j)}$ :

$$a_{nj} \stackrel{D}{=} \frac{1}{k} \sum_{l=1}^{c_{nj}} B_{kj} 2^{-l} + T$$

$$b_{nj} \stackrel{D}{=} \frac{1}{k} \sum_{l=1}^{c_{nj}} B_{kj} 2^{-l} + 2^{-c_{nj}} + T$$

No matter the value of  $T$ , the length of the  $j^{\text{th}}$  side of the box is given by:

$$\lambda(A_{nj}) = b_{nj} - a_{nj} = \frac{1}{k} 2^{-c_{nj}}$$

The division by the number of clusters  $k$  reflects the fact that the test point falls within a cluster of width  $\frac{1}{k}$ , so we divide the typical uniform  $[0,1]$  binary expansion by the same factor. The measure of the box  $A_n$  is therefore equal to

$$\begin{aligned} \lambda(A_n) &= \prod_{j=1}^S \lambda(A_{nj}) \\ &= \left(\frac{1}{k}\right)^S 2^{-\lceil \log_2 c_n \rceil} \end{aligned}$$

since by construction,  $\sum_j c_{nj} = \lceil \log_2 c_n \rceil$ .

The rest of the proof is structured as follows:

- (i) We derive the expression for the ratio of the *Ensemble* and *Merged* biases
- (ii) We derive expressions for the terms  $W_1 W_2'$  and  $H_1 H_2'$
- (iii) We use (ii) to factor the expressions for the *Ensemble* and *Merged* biases into two terms
- (iv) We provide upper and lower bounds for the first term of the factorization
- (v) We use these bounds to bound the overall limiting ratio
- (vi) We simplify the second term of the factorization
- (vii) We combine all previous steps and take limits to complete the proof

PROOF.

- (i) The leading term of the squared bias for the *Ensemble* can be represented as

$$\begin{aligned} & n(n-1) \mathbb{E}_{\mathbf{x}_*, \mathcal{D}_n} [\mathbb{E}_\theta [W_1] (f(\mathbf{x}_1) - f(\mathbf{x}_*)) \mathbb{E}_\theta [W_2] (f(\mathbf{x}_2) - f(\mathbf{x}_*))] \\ &= n(n-1) \mathbb{E}_{\mathbf{x}_*, \mathcal{D}_n} [\mathbb{E}_\theta [W_1] \mathbb{E}_\theta [W_2] (f(\mathbf{x}_1) - f(\mathbf{x}_*)) (f(\mathbf{x}_2) - f(\mathbf{x}_*))] \\ &= n(n-1) \mathbb{E}_{\mathbf{x}_*, \mathcal{D}_n, \theta, \theta'} [W_1 W_2' (f(\mathbf{x}_1) - f(\mathbf{x}_*)) (f(\mathbf{x}_2) - f(\mathbf{x}_*))] \end{aligned}$$

where  $W_i(\mathbf{x}_*, \theta) = \sum_{b=1}^k W_{ib}(\mathbf{x}_*, \theta)$ , as defined in Lemma 3.1 (i) and  $\theta'$  is an independent copy of  $\theta$ ; thus, for any quantity indexed with the  $'$  notation, we replace  $A_n(\mathbf{x}_*, \theta)$  with  $A_n(\mathbf{x}_*, \theta')$ .

The leading term of the squared bias for the *Merged* is equal to

$$\begin{aligned} & n(n-1)\mathbb{E}_{\mathbf{x}_*, \mathcal{D}_n} [\mathbb{E}_\theta [H_1] (f(\mathbf{x}_1) - f(\mathbf{x}_*)) \mathbb{E}_\theta [H_2] (f(\mathbf{x}_2) - f(\mathbf{x}_*))] \\ &= n(n-1)\mathbb{E}_{\mathbf{x}_*, \mathcal{D}_n, \theta, \theta'} \left[ H_1 H_2' (f(\mathbf{x}_1) - f(\mathbf{x}_*)) (f(\mathbf{x}_2) - f(\mathbf{x}_*)) \right] \end{aligned}$$

where  $H_1$  and  $H_2'$  are defined in Lemma 3.1 (ii).

Therefore, the limiting ratio of the *Ensemble* bias vs. the *Merged* bias is

$$\lim_{n \rightarrow \infty} \sqrt{\frac{\mathbb{E}_{\mathbf{x}_*, \mathcal{D}_n, \theta, \theta'} [W_1 W_2' (f(\mathbf{x}_1) - f(\mathbf{x}_*)) (f(\mathbf{x}_2) - f(\mathbf{x}_*))]}{\mathbb{E}_{\mathbf{x}_*, \mathcal{D}_n, \theta, \theta'} [H_1 H_2' (f(\mathbf{x}_1) - f(\mathbf{x}_*)) (f(\mathbf{x}_2) - f(\mathbf{x}_*))]}}$$

For the rest of the proof, we focus on evaluating the ratio within the square root, and applying the square root function as the last step.

(ii) To simplify this further, we expand the quantities  $W_1 W_2'$  and  $H_1 H_2'$ .

$$\begin{aligned} & W_1 W_2' \\ &= \mathbb{1}_{\{\mathbf{x}_1 \in A_n\}} \mathbb{1}_{\{\mathbf{x}_2 \in A'_n\}} \\ &\times \left[ \sum_{b=1}^k \frac{\mathbb{1}_{\{\mathbf{x}_1 \in [\frac{b-1}{k}, \frac{b}{k}]^S\}} \mathbb{1}_{\{\mathbf{x}_* \in [\frac{b-1}{k}, \frac{b}{k}]^S\}}}{N_b} \mathbb{1}_{\{\epsilon_{nb}\}} \right] \times \left[ \sum_{b=1}^k \frac{\mathbb{1}_{\{\mathbf{x}_1 \in [\frac{b-1}{k}, \frac{b}{k}]^S\}} \mathbb{1}_{\{\mathbf{x}_* \in [\frac{b-1}{k}, \frac{b}{k}]^S\}}}{N_b'} \mathbb{1}_{\{\epsilon'_{nb}\}} \right] \\ &= \mathbb{1}_{\{\mathbf{x}_1 \in A_n\}} \mathbb{1}_{\{\mathbf{x}_2 \in A'_n\}} \\ &\times \left[ \sum_{b=1}^k \frac{\mathbb{1}_{\{\mathbf{x}_1 \in [\frac{b-1}{k}, \frac{b}{k}]^S\}} \mathbb{1}_{\{\mathbf{x}_2 \in [\frac{b-1}{k}, \frac{b}{k}]^S\}} [\mathbb{1}_{\{\mathbf{x}_* \in [\frac{b-1}{k}, \frac{b}{k}]^S\}}]^2 \mathbb{1}_{\{\epsilon_{nb}\}} \mathbb{1}_{\{\epsilon'_{nb}\}}}{N_b N_b'} \right] \end{aligned}$$

The cross terms of the product are equal to 0, since  $\mathbf{x}_1, \mathbf{x}_1$ , and  $\mathbf{x}_*$  have to fall in the same cluster for any term to be non-zero.

Similarly,

$$H_1 H_2' = \mathbb{1}_{\{\mathbf{x}_1 \in A_n\}} \mathbb{1}_{\{\mathbf{x}_2 \in A'_n\}} \times \frac{\mathbb{1}_{\{\epsilon_n\}}}{N_n} \times \frac{\mathbb{1}_{\{\epsilon'_n\}}}{N'_n}$$

(iii) We now simplify these quantities using the following definitions and assumptions: Define

$$T_b = \sum_{i \geq 3} \mathbb{1}_{\{\mathbf{x}_i \in A_n\}} \mathbb{1}_{\{\mathbf{x}_i \in [\frac{b-1}{k}, \frac{b}{k}]^S\}} \mathbb{1}_{\{\mathbf{x}_* \in [\frac{b-1}{k}, \frac{b}{k}]^S\}}$$

for  $b = 1, \dots, k$  and let  $T'_b$  be the equivalent expressions based on  $\theta'$ . We make the assumption that the quantities  $\mathbb{1}_{\{\epsilon_{nb}\}}$ ,  $b = 1, \dots, k$ , as well as  $\mathbb{1}_{\{\epsilon_n\}}$ , are all non-zero; that is, that there is always at least one training point that falls within  $A_n(\mathbf{x}_*, \theta)$ , within the box (leaf node) containing the test point, regardless of the test point's true cluster assignment. Without loss of generality, we can therefore order the dataset so that one of  $\mathbf{x}_1, \mathbf{x}_2$  falls within  $A_n(\mathbf{x}_*, \theta)$  and the other falls in another cluster. For any test point, we can identify at least  $k$  training data points that belong to each distinct cluster out of which one is guaranteed to fall within the same leaf node as the test point. There are therefore a minimum of  $k/2$  different arrangements of the training set that meet this criteria for all  $b = 1, \dots, k$ .

For test points belonging to cluster  $b$ , we denote the event that this assumption is met by  $d_b = \mathbb{1}_{\{\epsilon_{nb} > 0, \sum_{i=1}^2 \mathbb{1}_{\{\mathbf{x}_i \in A_n\}} = 1, \sum_{i=1}^2 \mathbb{1}_{\{\mathbf{x}_i \in [\frac{b-1}{k}, \frac{b}{k}]^S\}} = 1\}}$ .

For any test point belonging to an arbitrary cluster, we denote the event that this assumption is met by  $d_n = \mathbb{1}_{\{\epsilon_n > 0, \sum_{i=1}^2 \mathbb{1}_{\{\mathbf{x}_i \in A_n\}} = 1\}}$ . This event is in fact exactly equivalent to our overall assumption, so by definition,  $P(\mathcal{D}_n) = 1$ . Therefore,

$$\mathbb{E} \left[ \frac{\mathbb{1}_{\{\epsilon_{nb}\}} \mathbb{1}_{\{\epsilon'_{nb}\}}}{N_b N_b'} \middle| \mathbf{x}_* \right] = \mathbb{E} \left[ \frac{1}{(1 + T_b)(1 + T'_b)} \middle| \mathbf{x}_*, d_b \right]$$

$$\begin{aligned}
&= \mathbb{E} \left[ \frac{1}{(1+T_b)(1+T'_b)} \middle| \mathbf{x}_\star \right] \\
&= \frac{k}{2} \mathbb{E} \left[ \frac{1}{(1+T_b)(1+T'_b)} \middle| \mathbf{x}_\star \right]
\end{aligned}$$

for  $b = 1, \dots, k$ . For the *Merged* learner, we can similarly define

$$U = \sum_{i \geq 3} \mathbb{1}_{\{\mathbf{x}_i \in A_n\}}$$

and

$$\begin{aligned}
\mathbb{E} \left[ \frac{\mathbb{1}_{\{\epsilon_n\}} \mathbb{1}_{\{\epsilon'_n\}}}{N_n N'_n} \middle| \mathbf{x}_\star \right] &= \mathbb{E} \left[ \frac{1}{(1+U)(1+U')} \middle| \mathbf{x}_\star, d_n \right] \\
&= \mathbb{E} \left[ \frac{1}{(1+U)(1+U')} \middle| \mathbf{x}_\star \right]
\end{aligned}$$

Given these definitions, we can further simplify the ratio of the squared biases:

$$\frac{\mathbb{E}_{\mathbf{x}_\star, \mathcal{D}_n, \theta, \theta'} [W_1 W'_2 (f(\mathbf{x}_1) - f(\mathbf{x}_\star))(f(\mathbf{x}_2) - f(\mathbf{x}_\star))]}{\mathbb{E}_{\mathbf{x}_\star, \mathcal{D}_n, \theta, \theta'} [H_1 H'_2 (f(\mathbf{x}_1) - f(\mathbf{x}_\star))(f(\mathbf{x}_2) - f(\mathbf{x}_\star))]}$$

(iia) The numerator (corresponding to the leading term of the squared bias of the *Ensemble*) simplifies to:

$$\begin{aligned}
&\mathbb{E}_{\mathbf{x}_\star, \mathcal{D}_n, \theta, \theta'} \left[ W_1 W'_2 (f(\mathbf{x}_1) - f(\mathbf{x}_\star))(f(\mathbf{x}_2) - f(\mathbf{x}_\star)) \right] \\
&= \mathbb{E}_{\mathbf{x}_\star, \mathcal{D}_n, \theta, \theta'} \left[ \mathbb{1}_{\{\mathbf{x}_1 \in A_n\}} \mathbb{1}_{\{\mathbf{x}_2 \in A'_n\}} \times \left[ \sum_{b=1}^k \frac{\mathbb{1}_{\{\mathbf{x}_1 \in [\frac{b-1}{k}, \frac{b}{k}]^S\}} \mathbb{1}_{\{\mathbf{x}_2 \in [\frac{b-1}{k}, \frac{b}{k}]^S\}} [\mathbb{1}_{\{\mathbf{x}_\star \in [\frac{b-1}{k}, \frac{b}{k}]^S\}}]^2 \mathbb{1}_{\{\epsilon_{nb}\}} \mathbb{1}_{\{\epsilon'_{nb}\}}}{N_b N'_b} \right] \right] \\
&= \mathbb{E}_{\mathbf{x}_\star, \mathcal{D}_n, \theta, \theta'} \left[ \mathbb{E} \left[ \mathbb{1}_{\{\mathbf{x}_1 \in A_n\}} \mathbb{1}_{\{\mathbf{x}_2 \in A'_n\}} \times k \left[ \frac{\mathbb{1}_{\{\mathbf{x}_1 \in [0, \frac{1}{k}]^S\}} \mathbb{1}_{\{\mathbf{x}_2 \in [0, \frac{1}{k}]^S\}} [\mathbb{1}_{\{\mathbf{x}_\star \in [0, \frac{1}{k}]^S\}}]^2 \mathbb{1}_{\{\epsilon_{n1}\}} \mathbb{1}_{\{\epsilon'_{n1}\}}}{N_1 N'_1} \right] \middle| \mathbf{x}_\star, \theta, \theta' \right] \right] \\
&= k \times \mathbb{E}_{\mathbf{x}_\star, \mathcal{D}_n} \left[ \mathbb{E} \left[ \frac{1}{(1+T_1)(1+T'_1)} \middle| \mathbf{x}_\star, \theta, \theta', d_b \right] \right. \\
&\quad \times \mathbb{E}_{\mathbf{x}_1, \mathbf{x}_2} \left[ \mathbb{1}_{\{\mathbf{x}_1 \in A_n\}} \mathbb{1}_{\{\mathbf{x}_2 \in A'_n\}} \mathbb{1}_{\{\mathbf{x}_1 \in [0, \frac{1}{k}]^S\}} \mathbb{1}_{\{\mathbf{x}_2 \in [0, \frac{1}{k}]^S\}} [\mathbb{1}_{\{\mathbf{x}_\star \in [0, \frac{1}{k}]^S\}}]^2 \right. \\
&\quad \left. \left. \times (f(\mathbf{x}_1) - f(\mathbf{x}_\star))(f(\mathbf{x}_2) - f(\mathbf{x}_\star)) \middle| \mathbf{x}_\star, \theta, \theta' \right] \right] \\
&= \frac{k^2}{2} \mathbb{E}_{\mathbf{x}_\star, \mathcal{D}_n} \left[ \mathbb{E} \left[ \frac{1}{(1+T_1)(1+T'_1)} \middle| \mathbf{x}_\star, \theta, \theta' \right] \right. \\
&\quad \left. \times \left( \mathbb{E}_{\mathbf{x}_1} \left[ \mathbb{1}_{\{\mathbf{x}_1 \in A_n\}} \mathbb{1}_{\{\mathbf{x}_1 \in [0, \frac{1}{k}]^S\}} \mathbb{1}_{\{\mathbf{x}_\star \in [0, \frac{1}{k}]^S\}} (f(\mathbf{x}_1) - f(\mathbf{x}_\star)) \middle| \mathbf{x}_\star \right] \right)^2 \right]
\end{aligned}$$

Various independence relations are used to simplify the expression:  $\mathbf{x}_1 \perp \mathbf{x}_2$ ,  $\theta \perp \theta'$ , and  $T_1 \perp \mathbf{x}_1, \mathbf{x}_2$ .

(iiib) The denominator (corresponding to the leading term of the squared bias of the *Merged*) simplifies to:

$$\begin{aligned}
& \mathbb{E}_{\mathbf{x}_*, \mathcal{D}_n, \theta, \theta'} \left[ H_1 H_2' (f(\mathbf{x}_1) - f(\mathbf{x}_*)) (f(\mathbf{x}_2) - f(\mathbf{x}_*)) \right] \\
& \mathbb{E}_{\mathbf{x}_*, \mathcal{D}_n, \theta, \theta'} \left[ \mathbb{1}_{\{\mathbf{x}_1 \in A_n\}} \mathbb{1}_{\{\mathbf{x}_2 \in A'_n\}} \left( \frac{1}{1+U} \right) \left( \frac{1}{1+U'} \right) (f(\mathbf{x}_1) - f(\mathbf{x}_*)) (f(\mathbf{x}_2) - f(\mathbf{x}_*)) \right] \\
& \mathbb{E}_{\mathbf{x}_*, \mathcal{D}_n, \theta} \left[ \left( \frac{1}{1+U} \right) \left( \frac{1}{1+U'} \right) (\mathbb{1}_{\{\mathbf{x}_1 \in A_n\}} (f(\mathbf{x}_1) - f(\mathbf{x}_*)))^2 \right] \\
& = \mathbb{E}_{\mathbf{x}_*, \mathcal{D}_n} \left[ \mathbb{E} \left[ \frac{1}{(1+U)(1+U')} \middle| \mathbf{x}_*, \theta, \theta' \right] \times (\mathbb{E}_{\mathbf{x}_1} [\mathbb{1}_{\{\mathbf{x}_1 \in A_n\}} (f(\mathbf{x}_1) - f(\mathbf{x}_*)) \middle| \mathbf{x}_*])^2 \right]
\end{aligned}$$

(iv) We now focus on calculating  $\mathbb{E} \left[ \frac{1}{(1+T_1)(1+T_1')} \middle| \mathbf{x}_*, \theta, \theta' \right]$  and  $\mathbb{E} \left[ \frac{1}{(1+U)(1+U')} \middle| \mathbf{x}_*, \theta, \theta' \right]$ . To upper bound these quantities, we use the fact that for  $Z \sim \text{Binomial}(m, p)$ ,  $\mathbb{E} \left[ \left( \frac{1}{1+Z} \right)^2 \right] \leq \frac{1}{(m+1)(m+2)p^2}$  along with the Cauchy-Schwarz inequality. To lower bound these quantities, we use the fact that for  $Z \sim \text{Binomial}(m, p)$ , one has that  $\mathbb{E} \left[ \frac{1}{1+Z} \right] = \frac{1}{(m+1)p} [1 - (1-p)^{m+1}]$  along with the definition of covariance, which tells us that  $\text{Cov}(X, Y) = E[XY] - E[X]E[Y] \Rightarrow E[X]E[Y] \leq E[XY]$  for positive  $\text{Cov}(X, Y)$ . To move forward, we need to calculate the binomial probabilities associated with  $T_1$  and  $U$ .  $T_1 \sim \text{Binomial}(n-2, p_e)$ , where

$$\begin{aligned}
p_e &= \mathbb{E} \left[ \mathbb{1}_{\{\mathbf{x}_i \in A_n\}} \mathbb{1}_{\{\mathbf{x}_i \in [0, \frac{1}{k}]^S\}} \mathbb{1}_{\{\mathbf{x}_* \in [0, \frac{1}{k}]^S\}} \right] \\
&= \mathbb{E} \left[ \mathbb{1}_{\{\mathbf{x}_i \in A_n\}} \middle| \mathbb{1}_{\{\mathbf{x}_i \in [0, \frac{1}{k}]^S\}} \mathbb{1}_{\{\mathbf{x}_* \in [0, \frac{1}{k}]^S\}} \right] \times \mathbb{E} \left[ \mathbb{1}_{\{\mathbf{x}_i \in [0, \frac{1}{k}]^S\}} \right] \times \mathbb{E} \left[ \mathbb{1}_{\{\mathbf{x}_* \in [0, \frac{1}{k}]^S\}} \right] \\
&= \frac{1}{k^2} \prod_{j=1}^S \frac{b_{nj} - a_{nj}}{\frac{1}{k}} \\
&= \frac{1}{k^2} 2^{-\lceil \log_2 c_n \rceil}
\end{aligned}$$

$U \sim \text{Binomial}(n-2, p_m)$  where

$$\begin{aligned}
p_m &= E_{\mathbf{x}_1} [\mathbb{1}_{\{\mathbf{x}_1 \in A_n\}}] \\
&= \prod_{j=1}^S k \times P \left( \mathbb{1}_{\{\mathbf{x}_1^{(j)} \in A_{n_j}\}} \middle| \mathbf{x}_1^{(j)} \in \left[ 0, \frac{1}{k} \right] \right) P \left( \mathbf{x}_1^{(j)} \in \left[ 0, \frac{1}{k} \right] \right) \\
&= \prod_{j=1}^S P \left( \mathbb{1}_{\{\mathbf{x}_1^{(j)} \in A_{n_j}\}} \middle| \mathbf{x}_1^{(j)} \in \left[ 0, \frac{1}{k} \right], \mathbf{x}_*^{(j)} \in \left[ 0, \frac{1}{k} \right] \right) P \left( \mathbf{x}_*^{(j)} \in \left[ 0, \frac{1}{k} \right] \right) \\
&= \prod_{j=1}^S \frac{b_{nj} - a_{nj}}{\frac{1}{k}} \times \frac{1}{k} \\
&= \frac{1}{k} 2^{-\lceil \log_2 c_n \rceil}
\end{aligned}$$

Now, we can state that by the definition of covariance,

$$\mathbb{E} \left[ \frac{1}{(1+T_1)(1+T_1')} \middle| \mathbf{x}_*, \theta, \theta' \right] \geq \mathbb{E} \left[ \frac{1}{(1+T_1)} \middle| \mathbf{x}_*, \theta, \theta' \right] \mathbb{E} \left[ \frac{1}{(1+T_1')} \middle| \mathbf{x}_*, \theta, \theta' \right]$$



$$\begin{aligned}
&= \left( \mathbb{E} \left[ \frac{1}{(1+T_1)} \middle| \mathbf{x}_*, \theta, \theta' \right] \right)^2 \\
&= \frac{k^4 4^{\lceil \log_2 c_n \rceil}}{(n-1)^2} \left[ 1 - \left( \frac{1}{k^2} 2^{-\lceil \log_2 c_n \rceil} \right)^{n-1} \right]^2
\end{aligned}$$

By the Cauchy-Schwarz inequality,

$$\begin{aligned}
&\mathbb{E} \left[ \frac{1}{(1+T_1)(1+T'_1)} \middle| \mathbf{x}_*, \theta, \theta' \right] \\
&\leq \sqrt{\mathbb{E} \left[ \left( \frac{1}{1+T_1} \right)^2 \middle| \mathbf{x}_*, \theta, \theta' \right]} \sqrt{\mathbb{E} \left[ \left( \frac{1}{1+T'_1} \right)^2 \middle| \mathbf{x}_*, \theta, \theta' \right]} \\
&= \left( \frac{k^2 2^{\lceil \log_2 c_n \rceil}}{\sqrt{n(n-1)}} \right)^2 \\
&= \frac{k^4 4^{\lceil \log_2 c_n \rceil}}{n(n-1)}
\end{aligned}$$

Putting it all together,

$$\frac{k^4 4^{\lceil \log_2 c_n \rceil}}{(n-1)^2} \left[ 1 - \left( \frac{1}{k^2} 2^{-\lceil \log_2 c_n \rceil} \right)^{n-1} \right]^2 \leq \mathbb{E} \left[ \frac{1}{(1+T_1)(1+T'_1)} \middle| \mathbf{x}_*, \theta, \theta' \right] \leq \frac{k^4 4^{\lceil \log_2 c_n \rceil}}{n(n-1)}$$

Now, we can do a similar calculation for  $\mathbb{E} \left[ \frac{1}{(1+U)(1+U')} \middle| \mathbf{x}_*, \theta, \theta' \right]$ , yielding:

$$\frac{k^2 4^{\lceil \log_2 c_n \rceil}}{(n-1)^2} \left[ 1 - \left( \frac{1}{k} 2^{-\lceil \log_2 c_n \rceil} \right)^{n-1} \right]^2 \leq \mathbb{E} \left[ \frac{1}{(1+U)(1+U')} \middle| \mathbf{x}_*, \theta, \theta' \right] \leq \frac{k^2 4^{\lceil \log_2 c_n \rceil}}{n(n-1)}$$

(v) To get an upper bound on our ratio simplified in part (iii), we can take the max of the numerator and the min of the denominator:

$$\begin{aligned}
&\frac{\frac{k^2}{2} \mathbb{E}_{\mathbf{x}_*, \mathcal{D}_n} \left[ \mathbb{E} \left[ \frac{1}{(1+T_1)(1+T'_1)} \middle| \mathbf{x}_*, \theta, \theta' \right] \times \left( \mathbb{E}_{\mathbf{x}_1} \left[ \mathbb{1}_{\{\mathbf{x}_1 \in A_n\}} \mathbb{1}_{\{\mathbf{x}_1 \in [0, \frac{1}{k}]^S\}} \mathbb{1}_{\{\mathbf{x}_* \in [0, \frac{1}{k}]^S\}} (f(\mathbf{x}_1) - f(\mathbf{x}_*)) \middle| \mathbf{x}_* \right] \right)^2 \right]}{\mathbb{E}_{\mathbf{x}_*, \mathcal{D}_n} \left[ \mathbb{E} \left[ \frac{1}{(1+U)(1+U')} \middle| \mathbf{x}_*, \theta, \theta' \right] \left( \mathbb{E}_{\mathbf{x}_1} \left[ \mathbb{1}_{\{\mathbf{x}_1 \in A_n\}} (f(\mathbf{x}_1) - f(\mathbf{x}_*)) \middle| \mathbf{x}_* \right] \right)^2 \right]} \\
&= \frac{\frac{k^2}{2} \mathbb{E}_{\mathbf{x}_*, \mathcal{D}_n} \left[ \frac{k^4 4^{\lceil \log_2 c_n \rceil}}{n(n-1)} \left( \mathbb{E}_{\mathbf{x}_1} \left[ \mathbb{1}_{\{\mathbf{x}_1 \in A_n\}} \mathbb{1}_{\{\mathbf{x}_1 \in [0, \frac{1}{k}]^S\}} \mathbb{1}_{\{\mathbf{x}_* \in [0, \frac{1}{k}]^S\}} (f(\mathbf{x}_1) - f(\mathbf{x}_*)) \middle| \mathbf{x}_* \right] \right)^2 \right]}{\mathbb{E}_{\mathbf{x}_*, \mathcal{D}_n} \left[ \frac{k^2 4^{\lceil \log_2 c_n \rceil}}{(n-1)^2} \left[ 1 - \left( \frac{1}{k} 2^{-\lceil \log_2 c_n \rceil} \right)^{n-1} \right]^2 \left( \mathbb{E}_{\mathbf{x}_1} \left[ \mathbb{1}_{\{\mathbf{x}_1 \in A_n\}} (f(\mathbf{x}_1) - f(\mathbf{x}_*)) \middle| \mathbf{x}_* \right] \right)^2 \right]} \\
&= \left( \frac{k^4}{2} \right) \left( \frac{n-1}{n} \right) \left( \frac{1}{\left[ 1 - \left( \frac{1}{k} 2^{-\lceil \log_2 c_n \rceil} \right)^{n-1} \right]^2} \right)
\end{aligned}$$

$$\mathbb{E}_{\mathbf{x}_*, \mathcal{D}_n} \left[ \left( \mathbb{E}_{\mathbf{x}_1} \left[ \mathbb{1}_{\{\mathbf{x}_1 \in A_n\}} \mathbb{1}_{\{\mathbf{x}_1 \in [0, \frac{1}{k}]^S\}} \mathbb{1}_{\{\mathbf{x}_* \in [0, \frac{1}{k}]^S\}} (f(\mathbf{x}_1) - f(\mathbf{x}_*)) \middle| \mathbf{x}_* \right] \right)^2 \right] \\ \times \frac{1}{\mathbb{E}_{\mathbf{x}_*, \mathcal{D}_n} \left[ \left( \mathbb{E}_{\mathbf{x}_1} \left[ \mathbb{1}_{\{\mathbf{x}_1 \in A_n\}} (f(\mathbf{x}_1) - f(\mathbf{x}_*)) \middle| \mathbf{x}_* \right] \right)^2 \right]}$$

We find the lower bound of the ratio by taking the min of the numerator and max of the denominator, yielding:

$$\frac{\frac{k^2}{2} \mathbb{E}_{\mathbf{x}_*, \mathcal{D}_n} \left[ \times \left( \mathbb{E}_{\mathbf{x}_1} \left[ \mathbb{1}_{\{\mathbf{x}_1 \in A_n\}} \mathbb{1}_{\{\mathbf{x}_1 \in [0, \frac{1}{k}]^S\}} \mathbb{1}_{\{\mathbf{x}_* \in [0, \frac{1}{k}]^S\}} (f(\mathbf{x}_1) - f(\mathbf{x}_*)) \middle| \mathbf{x}_* \right] \right)^2 \right]}{\min \frac{\mathbb{E}_{\mathbf{x}_*, \mathcal{D}_n} \left[ \mathbb{E} \left[ \frac{1}{(1+U)(1+U')} \middle| \mathbf{x}_*, \theta, \theta' \right] \left( \mathbb{E}_{\mathbf{x}_1} \left[ \mathbb{1}_{\{\mathbf{x}_1 \in A_n\}} (f(\mathbf{x}_1) - f(\mathbf{x}_*)) \middle| \mathbf{x}_* \right] \right)^2 \right]}{\mathbb{E}_{\mathbf{x}_*, \mathcal{D}_n} \left[ \mathbb{E} \left[ \frac{1}{(1+U)(1+U')} \middle| \mathbf{x}_*, \theta, \theta' \right] \left( \mathbb{E}_{\mathbf{x}_1} \left[ \mathbb{1}_{\{\mathbf{x}_1 \in A_n\}} (f(\mathbf{x}_1) - f(\mathbf{x}_*)) \middle| \mathbf{x}_* \right] \right)^2 \right]}} \\ = \left( \frac{k^4}{2} \right) \left( \frac{n}{n-1} \right) \left[ 1 - \left( \frac{1}{k^2} 2^{-\lceil \log_2 c_n \rceil} \right)^{n-1} \right]^2 \\ \times \frac{\mathbb{E}_{\mathbf{x}_*, \mathcal{D}_n} \left[ \left( \mathbb{E}_{\mathbf{x}_1} \left[ \mathbb{1}_{\{\mathbf{x}_1 \in A_n\}} \mathbb{1}_{\{\mathbf{x}_1 \in [0, \frac{1}{k}]^S\}} \mathbb{1}_{\{\mathbf{x}_* \in [0, \frac{1}{k}]^S\}} (f(\mathbf{x}_1) - f(\mathbf{x}_*)) \middle| \mathbf{x}_* \right] \right)^2 \right]}{\mathbb{E}_{\mathbf{x}_*, \mathcal{D}_n} \left[ \left( \mathbb{E}_{\mathbf{x}_1} \left[ \mathbb{1}_{\{\mathbf{x}_1 \in A_n\}} (f(\mathbf{x}_1) - f(\mathbf{x}_*)) \middle| \mathbf{x}_* \right] \right)^2 \right]}$$

(vi) We now simplify the quantity

$$\frac{\mathbb{E}_{\mathbf{x}_*, \mathcal{D}_n} \left[ \left( \mathbb{E}_{\mathbf{x}_1} \left[ \mathbb{1}_{\{\mathbf{x}_1 \in A_n\}} \mathbb{1}_{\{\mathbf{x}_1 \in [0, \frac{1}{k}]^S\}} \mathbb{1}_{\{\mathbf{x}_* \in [0, \frac{1}{k}]^S\}} (f(\mathbf{x}_1) - f(\mathbf{x}_*)) \middle| \mathbf{x}_* \right] \right)^2 \right]}{\mathbb{E}_{\mathbf{x}_*, \mathcal{D}_n} \left[ \left( \mathbb{E}_{\mathbf{x}_1} \left[ \mathbb{1}_{\{\mathbf{x}_1 \in A_n\}} (f(\mathbf{x}_1) - f(\mathbf{x}_*)) \middle| \mathbf{x}_* \right] \right)^2 \right]}$$

We begin with the numerator, evaluating the expression within the inner expectation:

$$\mathbb{E}_{\mathbf{x}_1} \left[ \mathbb{1}_{\{\mathbf{x}_1 \in A_n\}} \mathbb{1}_{\{\mathbf{x}_1 \in [0, \frac{1}{k}]^S\}} \mathbb{1}_{\{\mathbf{x}_* \in [0, \frac{1}{k}]^S\}} (f(\mathbf{x}_1) - f(\mathbf{x}_*)) \middle| \mathbf{x}_* \right] \\ = \mathbb{E}_{\mathbf{x}_1} \left[ (f(\mathbf{x}_1) - f(\mathbf{x}_*)) \middle| \mathbf{x}_1 \in A_n, \mathbf{x}_1 \in \left[ 0, \frac{1}{k} \right]^S, \mathbf{x}_* \in \left[ 0, \frac{1}{k} \right]^S, \mathbf{x}_* \right] \\ \times \mathbb{E} \left[ \mathbb{1}_{\{\mathbf{x}_1 \in A_n\}} \middle| \mathbf{x}_1 \in \left[ 0, \frac{1}{k} \right]^S, \mathbf{x}_* \in \left[ 0, \frac{1}{k} \right]^S, \mathbf{x}_* \right] \times \mathbb{E} \left[ \mathbb{1}_{\{\mathbf{x}_1 \in [0, \frac{1}{k}]^S\}} \right] \times \mathbb{E} \left[ \mathbb{1}_{\{\mathbf{x}_* \in [0, \frac{1}{k}]^S\}} \right] \\ = \left( \frac{\lambda(A_n)}{k} \right) \mathbb{E}_{\mathbf{x}_1} \left[ (f(\mathbf{x}_1) - f(\mathbf{x}_*)) \middle| \mathbf{x}_1 \in A_n, \mathbf{x}_* \right]$$

Moving onto the denominator, we again evaluate the expression within the inner expectation:

$$\mathbb{E}_{\mathbf{x}_1} \left[ \mathbb{1}_{\{\mathbf{x}_1 \in A_n\}} (f(\mathbf{x}_1) - f(\mathbf{x}_*)) \middle| \mathbf{x}_* \right] \\ = \mathbb{E}_{\mathbf{x}_1} \left[ (f(\mathbf{x}_1) - f(\mathbf{x}_*)) \middle| \mathbf{x}_1 \in A_n, \mathbf{x}_* \right] \times \mathbb{E} \left[ \mathbb{1}_{\{\mathbf{x}_1 \in A_n\}} \middle| \mathbf{x}_* \right] \\ = \mathbb{E}_{\mathbf{x}_1} \left[ (f(\mathbf{x}_1) - f(\mathbf{x}_*)) \middle| \mathbf{x}_1 \in A_n, \mathbf{x}_* \right] \frac{\lambda(A_n)}{\frac{1}{k}}$$

Therefore,

$$\begin{aligned}
& \frac{\mathbb{E}_{\mathbf{x}_*, \mathcal{D}_n} \left[ \left( \mathbb{E}_{\mathbf{x}_1} \left[ \mathbb{1}_{\{\mathbf{x}_1 \in A_n\}} \mathbb{1}_{\{\mathbf{x}_1 \in [0, \frac{1}{k}]^S\}} \mathbb{1}_{\{\mathbf{x}_* \in [0, \frac{1}{k}]^S\}} (f(\mathbf{x}_1) - f(\mathbf{x}_*)) \middle| \mathbf{x}_* \right] \right)^2 \right]}{\mathbb{E}_{\mathbf{x}_*, \mathcal{D}_n} \left[ \left( \mathbb{E}_{\mathbf{x}_1} \left[ \mathbb{1}_{\{\mathbf{x}_1 \in A_n\}} (f(\mathbf{x}_1) - f(\mathbf{x}_*)) \middle| \mathbf{x}_* \right] \right)^2 \right]} \\
&= \frac{\left( \frac{\lambda(A_n)}{k} \right)^2 \mathbb{E}_{\mathbf{x}_*, \mathcal{D}_n} \left[ \left( \mathbb{E}_{\mathbf{x}_1} \left[ f(\mathbf{x}_1) - f(\mathbf{x}_*) \middle| \mathbf{x}_1 \in A_n, \mathbf{x}_* \right] \right)^2 \right]}{(k\lambda(A_n))^2 \mathbb{E}_{\mathbf{x}_*, \mathcal{D}_n} \left[ \left( \mathbb{E}_{\mathbf{x}_1} \left[ f(\mathbf{x}_1) - f(\mathbf{x}_*) \middle| \mathbf{x}_1 \in A_n, \mathbf{x}_* \right] \right)^2 \right]} \\
&= \frac{1}{k^4}
\end{aligned}$$

Note that we do not need to make any assumptions on the form that  $f(x)$  takes, since the expressions involving the outcome model cancel between numerator and denominator.

(vii) Putting everything together from parts (v) and (vi),

$$\begin{aligned}
& \frac{\frac{k^2}{2} \mathbb{E}_{\mathbf{x}_*, \mathcal{D}_n} \left[ \times \left( \mathbb{E}_{\mathbf{x}_1} \left[ \mathbb{1}_{\{\mathbf{x}_1 \in A_n\}} \mathbb{1}_{\{\mathbf{x}_1 \in [0, \frac{1}{k}]^S\}} \mathbb{1}_{\{\mathbf{x}_* \in [0, \frac{1}{k}]^S\}} (f(\mathbf{x}_1) - f(\mathbf{x}_*)) \middle| \mathbf{x}_* \right] \right)^2 \right]}{\mathbb{E}_{\mathbf{x}_*, \mathcal{D}_n} \left[ \mathbb{E} \left[ \frac{1}{(1+U)(1+U')} \middle| \mathbf{x}_*, \theta, \theta' \right] \left( \mathbb{E}_{\mathbf{x}_1} \left[ \mathbb{1}_{\{\mathbf{x}_1 \in A_n\}} (f(\mathbf{x}_1) - f(\mathbf{x}_*)) \middle| \mathbf{x}_* \right] \right)^2 \right]} \\
&\geq \left( \frac{k^4}{2} \right) \left( \frac{n}{n-1} \right) \left[ 1 - \left( \frac{1}{k^2} 2^{-\lceil \log_2 c_n \rceil} \right)^{n-1} \right]^2 \times \frac{1}{k^4} \\
&= \left( \frac{n}{n-1} \right) \frac{1}{2} \left[ 1 - \left( \frac{1}{k^2} 2^{-\lceil \log_2 c_n \rceil} \right)^{n-1} \right]^2
\end{aligned}$$

and

$$\begin{aligned}
& \frac{\frac{k^2}{2} \mathbb{E}_{\mathbf{x}_*, \mathcal{D}_n} \left[ \times \left( \mathbb{E}_{\mathbf{x}_1} \left[ \mathbb{1}_{\{\mathbf{x}_1 \in A_n\}} \mathbb{1}_{\{\mathbf{x}_1 \in [0, \frac{1}{k}]^S\}} \mathbb{1}_{\{\mathbf{x}_* \in [0, \frac{1}{k}]^S\}} (f(\mathbf{x}_1) - f(\mathbf{x}_*)) \middle| \mathbf{x}_* \right] \right)^2 \right]}{\mathbb{E}_{\mathbf{x}_*, \mathcal{D}_n} \left[ \mathbb{E} \left[ \frac{1}{(1+U)(1+U')} \middle| \mathbf{x}_*, \theta, \theta' \right] \left( \mathbb{E}_{\mathbf{x}_1} \left[ \mathbb{1}_{\{\mathbf{x}_1 \in A_n\}} (f(\mathbf{x}_1) - f(\mathbf{x}_*)) \middle| \mathbf{x}_* \right] \right)^2 \right]} \\
&\leq \left( \frac{k^4}{2} \right) \left( \frac{n-1}{n} \right) \times \frac{1}{k^4} \left( \frac{1}{\left[ 1 - \left( \frac{1}{k} 2^{-\lceil \log_2 c_n \rceil} \right)^{n-1} \right]^2} \right) \\
&= \left( \frac{n}{n-1} \right) \frac{1}{2} \left( \frac{1}{\left[ 1 - \left( \frac{1}{k} 2^{-\lceil \log_2 c_n \rceil} \right)^{n-1} \right]^2} \right)
\end{aligned}$$

We now take square roots of the minimum and maximum values calculated above since we are interested in the ratio of the *Ensemble* bias vs. the *Merged* bias (not the squared ratio), and take limits as  $n \rightarrow \infty$ .

$$\begin{aligned}
\lim_{n \rightarrow \infty} \frac{\text{Ensemble bias}}{\text{Merged bias}} &\in \left[ \lim_{n \rightarrow \infty} \sqrt{\left(\frac{n}{n-1}\right) \frac{1}{2} \left[1 - \left(\frac{1}{k^2} 2^{-\lceil \log_2 c_n \rceil}\right)^{n-1}\right]^2}, \right. \\
&\left. \lim_{n \rightarrow \infty} \sqrt{\left(\frac{n}{n-1}\right) \frac{1}{2} \left(\frac{1}{\left[1 - \left(\frac{1}{k^2} 2^{-\lceil \log_2 c_n \rceil}\right)^{n-1}\right]^2}\right)} \right] \\
&\rightarrow \left[ \sqrt{\frac{1}{2}}, \sqrt{\frac{1}{2}} \right] \\
&\Rightarrow \lim_{n \rightarrow \infty} \frac{\text{Ensemble bias}}{\text{Merged bias}} \rightarrow \frac{1}{\sqrt{2}}
\end{aligned}$$

for any  $k \geq 2$

□

REMARK A.2. *Convergence of bias terms*

(i) *From the proof of Theorem 1, we can express the squared bias of the Ensemble as:*

$$\begin{aligned}
&n(n-1) \mathbb{E}_{\mathbf{x}_*, \mathcal{D}_n, \theta, \theta'} \left[ W_1 W_2' (f(\mathbf{x}_1) - f(\mathbf{x}_*)) (f(\mathbf{x}_2) - f(\mathbf{x}_*)) \right] \\
&\rightarrow \frac{k^{4-2S}}{2} \mathbb{E}_{\mathbf{x}_*, \mathcal{D}_n} \left[ \left( \mathbb{E}_{\mathbf{x}_1} \left[ f(\mathbf{x}_1) - f(\mathbf{x}_*) \mid \mathbf{x}_1 \in A_n, \mathbf{x}_* \right] \right)^2 \right] \\
&\geq O\left(\frac{1}{n}\right)
\end{aligned}$$

*The convergence of this term depends on the function  $f(x)$ , distributions of  $\mathbf{x}_1$  and  $\mathbf{x}_*$ , number of non-sparse variables  $S$ , the number of clusters  $k$ , and the total number of splits  $c_n$  (which influences the size of the box containing  $\mathbf{x}_*$ ). Assuming that  $\frac{k}{n}$ ,  $\frac{c_n}{n}$ , and  $\frac{S}{n} \rightarrow 0$  as  $n \rightarrow \infty$ , the squared bias converges at a rate greater than  $O\left(\frac{1}{n}\right)$*

(ii) *We can express the squared bias of the Merged as:*

$$\begin{aligned}
&n(n-1) \mathbb{E}_{\mathbf{x}_*, \mathcal{D}_n, \theta, \theta'} \left[ H_1 H_2' (f(\mathbf{x}_1) - f(\mathbf{x}_*)) (f(\mathbf{x}_2) - f(\mathbf{x}_*)) \right] \\
&\rightarrow k^{4-2S} \mathbb{E}_{\mathbf{x}_*, \mathcal{D}_n} \left[ \left( \mathbb{E}_{\mathbf{x}_1} \left[ f(\mathbf{x}_1) - f(\mathbf{x}_*) \mid \mathbf{x}_1 \in A_n, \mathbf{x}_* \right] \right)^2 \right] \\
&\geq O\left(\frac{1}{n}\right)
\end{aligned}$$

*using similar arguments as above.*

## A.2 Lemma A.3

We now show that the variance of the *Ensemble* and *Merged* asymptotically converge to zero. We assume that  $\text{Var}[f(\mathbf{x})|\mathbf{x}] \leq \sigma^2$  for some  $\sigma > 0$ .

LEMMA A.3. (i) *Using [Biau 2012, Proposition 2], we can express the variance of the Ensemble as*

$$\begin{aligned}
\mathbb{E}[\hat{Y}_E(\mathbf{x}_*) - \mathbb{E}[\hat{Y}_E(\mathbf{x}_*)|\mathbf{x}_*]]^2 &= n\sigma^2 \mathbb{E} \left[ \mathbb{E}_{\theta, \theta'} \left[ W_1 W_2' \right] \right] \\
&= n\sigma^2 \frac{k^2}{2} \mathbb{E}_{\mathbf{x}_*, \mathcal{D}_n} \left[ \mathbb{E} \left[ \frac{1}{(1+T_1)(1+T_1')} \mid \mathbf{x}_*, \theta, \theta' \right] \right]
\end{aligned}$$

$$\begin{aligned}
& \times \left( \mathbb{E}_{\mathbf{x}_1} \left[ \mathbb{1}_{\{\mathbf{x}_1 \in A_n\}} \mathbb{1}_{\{\mathbf{x}_1 \in [0, \frac{1}{k}]^S\}} \mathbb{1}_{\{\mathbf{x}_* \in [0, \frac{1}{k}]^S\}} \middle| \mathbf{x}_* \right] \right)^2 \\
& = n\sigma^2 \frac{k^2 k^4 4^{\lceil \log_2 c_n \rceil}}{2 n(n-1)} \left( \frac{\lambda(A_n)}{\frac{1}{k}} \left( \frac{1}{k} \right)^2 \right)^2 \\
& = \frac{\sigma^2 k^{(4-2S)}}{2(n-1)} \\
& = O\left(\frac{1}{n}\right)
\end{aligned}$$

using calculations from the proof of Theorem 1, step (iiia), (iv), and (vi) and finite assumptions on  $S$  and  $k$  outlined in Remark A.2. Note that we do NOT need a finite assumption on the number of total splits  $c_n$  for the variance to be  $O(1/n)$ .

(ii) Similarly, we can express the variance of the Merged as

$$\begin{aligned}
& \mathbb{E}[\hat{Y}_M(\mathbf{x}_*) - \mathbb{E}[\hat{Y}_M(\mathbf{x}_*) | \mathbf{x}_*]]^2 \\
& = n\sigma^2 \mathbb{E} \left[ \mathbb{E}_{\theta, \theta'} \left[ H_1 H_2' \right] \right] \\
& = n\sigma^2 \mathbb{E}_{\mathbf{x}_*, \mathcal{D}_n} \left[ \mathbb{E} \left[ \frac{1}{(1+U)(1+U')} \middle| \mathbf{x}_*, \theta, \theta' \right] \times \left( \mathbb{E}_{\mathbf{x}_1} \left[ \mathbb{1}_{\{\mathbf{x}_1 \in A_n\}} \middle| \mathbf{x}_* \right] \right)^2 \right] \\
& = n\sigma^2 \frac{k^2 4^{\lceil \log_2 c_n \rceil}}{n(n-1)} \left( \frac{\lambda(A_n)}{\frac{1}{k}} \right)^2 \\
& = \frac{\sigma^2 k^{(3-2S)}}{n-1} \\
& = O\left(\frac{1}{n}\right)
\end{aligned}$$

using calculations from the proof of Theorem 3.2, step (iiib), (iv), and (vi).

Therefore, the variance terms converge to 0 as  $n \rightarrow \infty$  and the squared bias asymptotically dominates the MSE.